Ecological Modelling 368 (2018) 357–376

Contents lists available at ScienceDirect

Ecological Modelling

journal homepage: www.elsevier.com/locate/ecolmodel

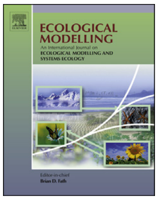

A high-resolution modeling study on diel and seasonal vertical migrations of high-latitude copepods

Kanchana Bandara[a,b,*], Øystein Varpe[b,c], Rubao Ji[d], Ketil Eiane[a]

[a] Faculty of Biosciences and Aquaculture, Nord University, 8049, Bodø, Norway
[b] The University Centre in Svalbard, 9171, Longyearbyen, Norway
[c] Akvaplan-niva, Fram Centre, 9296, Tromsø, Norway
[d] Woods Hole Oceanographic Institution, Redfield 2-14, Woods Hole, MA 02543, USA

ARTICLE INFO

Article history:
Received 20 September 2017
Received in revised form
12 December 2017
Accepted 12 December 2017
Available online 26 December 2017

Keywords:
Vertical migration
Seasonality
Phenology
Optimization model
Genetic algorithm
Habitat choice

ABSTRACT

Despite diel and seasonal vertical migrations (DVM and SVM) of high-latitude zooplankton have been studied since the late-19th century, questions still remain about the influence of environmental seasonality on vertical migration, and the combined influence of DVM and SVM on zooplankton fitness. Toward addressing these, we developed a model for simulating DVM and SVM of high-latitude herbivorous copepods in high spatio-temporal resolution. In the model, a unique timing and amplitude of DVM and SVM and its ontogenetic trajectory were defined as a vertical strategy. Growth, survival and reproductive performances of numerous vertical strategies hardwired to copepods spawned in different times of the year were assessed by a fitness estimate, which was heuristically maximized by a Genetic Algorithm to derive the optimal vertical strategy for a given model environment. The modelled food concentration, temperature and visual predation risk had a significant influence on the observed vertical strategies. Under low visual predation risk, DVM was less pronounced, and SVM and reproduction occurred earlier in the season, where capital breeding played a significant role. Reproduction was delayed by higher visual predation risk, and copepods that spawned later in the season used the higher food concentrations and temperatures to attain higher growth, which was efficiently traded off for survival through DVM. Consequently, the timing of SVM did not change much from that predicted under lower visual predation risk, but the body and reserve sizes of overwintering stages and the importance of capital breeding diminished. Altogether, these findings emphasize the significance of DVM in environments with elevated visual predation risk and shows its contrasting influence on the phenology of reproduction and SVM, and moreover highlights the importance of conducting field and modeling work to study these migratory strategies in concert.

1. Introduction

Vertical migration is a common behavior of many zooplankton taxa. Based on the periodicity, vertical migrations of high-latitude zooplankton are classified into diel and seasonal components, which have been studied since the late-19th century (reviewed in Russell, 1927; Cushing, 1951; Banse, 1964). The short-term diel vertical migration (DVM) has a periodicity of up to 24 h, and is understood as a strategy that trades off growth potential to reduce the mortality risk imposed by visual predators (Lampert, 1989; Ohman, 1990; Loose and Dawidowicz, 1994). The long-term seasonal vertical migration (SVM) has a periodicity of up to one year, and reflects adaptations to seasonal extremities of food availability (Head and Harris, 1985; Hind et al., 2000; Bandara et al., 2016), temperature (Hirche, 1991; Astthorsson and Gislason, 2003) and predation risk (Kaartvedt, 1996; Bagøien et al., 2000; Varpe and Fiksen, 2010). In either case, since both DVM and SVM can alter feeding, growth, survival and reproduction, and ultimately affect fitness (Aidley, 1981; Alerstam et al., 2003; Cresswell et al., 2011; Litchman et al., 2013), these migratory strategies are termed vertical strategies (Bandara et al., 2016).

Empirical knowledge on zooplankton vertical strategies largely comes from studying the dynamic vertical positioning of populations in a water column, and are often rather coarse in spatial (vertical) and temporal resolution (Pearre, 1979). This can undermine the key concept that such migrations are individual responses

---

* Corresponding author at: Faculty of Biosciences and Aquaculture, Nord University, 8049, Bodø, Norway.
E-mail addresses: kanchana.bandara@nord.no, kanchana_bandara@live.com (K. Bandara).

https://doi.org/10.1016/j.ecolmodel.2017.12.010

Table 1
Some endogenous and exogenous cues that are believed to proximately or ultimately regulate diel and seasonal vertical migrations of marine and freshwater zooplankton. Literature do not come from an exhaustive review and only serve as examples.

Cue	DVM	SVM
Temperature	McLaren (1963), Enright (1977)	Hirche (1991), Heath and Jónasdóttir (1999), Astthorsson and Gislason (2003)
Light (absolute or relative irradiance from sun, moon, stars, or aurora borealis, photoperiod, spectral quality, polarization etc.)	Clarke (1933), Gliwicz (1986), Frank and Widder (1997), Berge et al. (2009), Båtnes et al. (2015), Cohen et al. (2015), Bianchi and Mislan (2016), Bozman et al. (2017)	Sømme (1934), Ussing (1938), Miller et al. (1991)
Dissolved oxygen	Devol (1981), Bianchi et al. (2013)	–
Water depth, transparency and UV radiation	Rhode et al. (2001), Williamson et al. (2011), Ekvall et al. (2015)	Dupont and Aksnes (2012)
Tides, currents and advective transport	Hardy (1935), Wroblewski (1982), Kimmerer and McKinnon (1987)	Berge et al. (2012), Irigoien (2004)
Food availability	Hardy and Gunther (1935), Huntley and Brooks (1982), George (1983), Johnsen and Jakobsen (1987)	Herman (1983), Hind et al. (2000), Head and Harris (1985), Bandara et al. (2016)
Visual and tactile predation	Zaret and Suffern (1976), Iwasa (1982), Ohman (1990), Bollens et al. (1992), Loose and Dawidowicz (1994)	Kaartvedt (1996), Kaartvedt (2000), Dale et al. (1999), Bagøien et al. (2000), Varpe and Fiksen (2010)
Body size, ontogeny and pigmentation	Zaret and Kerfoot (1975), Uye et al. (1990), Hays et al. (1994), Dale and Kaartvedt (2000)	Østvedt (1955), Hind et al. (2000)
Nutritional state and lipid reserves	Fiksen and Carlotti (1998), Sekino and Yamamura (1999)	Visser and Jónasdóttir (1999), Thorisson (2006)
Endogenous rhythms and internal biological clocks	Cohen and Forward (2009), van Haren and Compton (2013)	Carlisle and Pitman (1961), Miller et al. (1991), Hirche (1996)

to certain cues or stimuli and not a property of the population (Zink, 2002), and may complicate the understanding of the relationships between vertical strategies and environmental variables (see Table 1 for examples). Moreover, since diel and seasonal vertical migrations occur on different spatial and temporal scales, studying these migrations together in the field in adequate resolution remains a major challenge. Although novel optical and acoustic methods of *in-situ* observation offer a solution to some of these problems (e.g. Basedow et al., 2010; Sainmont et al., 2014b; Bozman et al., 2017; Darnis et al., 2017), long-term deployment and accurately resolving the identity of the migrants remain as key challenges.

Mechanistic models offer an alternative means of studying zooplankton vertical strategies in higher resolution. Models related to DVM usually encompass the highest spatial ($\leq$1 m), temporal ($\leq$1 h) and biological (=individual) resolution (e.g. Fiksen and Giske, 1995; Eiane and Parisi, 2001; Liu et al., 2003; Burrows and Tarling, 2004; Hansen and Visser, 2016). Models related to SVM and diapause (i.e. hibrnation in deeper waters, e.g. Hirche, 1996) encompass the same biological resolution, but are usually coarse in spatio-temporal resolution. Here, the time intervals range from 1 h to 1d and vertical spatial elements are usually resolved to either absolute depth units (e.g. 1 m bins) or segregated habitats (e.g. Fiksen and Carlotti, 1998; Miller et al., 1998; Hind et al., 2000; Ji, 2011; Ji et al., 2012; Sainmont et al., 2015; Banas et al., 2016). The choice of a coarser spatio-temporal resolution of these models reflects the broader space and time scales at which the SVM and diapause occurs. This contrasting spatio-temporal scale makes it difficult to harbor lifetime dynamics of DVM to be simulated in SVM models without significantly increasing computer time. Consequently, most models that simulate SVM tend to either fully (e.g. Hind et al., 2000) or partly (i.e. of younger developmental stages, e.g. Fiksen and Carlotti, 1998) disregard DVM. However, the validity of such simplifications are questionable, given the geographically and taxonomically widespread nature of zooplankton DVM behavior and its ontogenetic patterns (Huntley and Brooks, 1982; Huang et al., 1993; Osgood and Frost, 1994; Hays, 1995). It is thus interesting to investigate whether the extra biological information resulting from modeling DVM and SVM in concert is a worthy trade-off for the elevated computer time. If so, such models may lead to improvements of the current understanding about how environmental seasonality shapes up vertical strategies, and the means of which the latter influences life histories of high latitude zooplankton.

Table 2
Evolvable (soft) parameters optimized in the model. The first six are proxies that define the vertical strategy. Vertical strategies of copepods spawned in different times of the year (t_B) are optimized using the GA.

Term	Definition	Range	Interval	Unit
α	Light sensitivity parameter	0–I_{max}[a]	1	μmol m^{-2} s^{-1}
β	Size-specificity of light sensitivity parameter	0–10	1	dim.less
γ	Growth allocation parameter	0–1	0.01	dim.less
δ	Seasonal descent parameter	0–1	0.01	dim.less
ζ	Overwintering depth	1–500	10	m
ε	Seasonal ascent parameter	0–1	0.01	dim.less
t_B	Time of birth[b]	1–8760	1	h

[a] The upper limit of α changes with the maximum surface irradiance of the model environment, i.e. I_{max} = 1500 μmol m^{-2} s^{-1} for Environment-L, 1300 μmol m^{-2} s^{-1} for Environment-M and 1100 μmol m^{-2} s^{-1} for Environment-H (cf. Fig. 1).

[b] Time of being spawned.

In this study, we present a model of zooplankton vertical strategies. The model operates in a high-latitude setting and simulates both DVM and SVM of a herbivorous copepod with an annual life cycle in high spatial (vertical) and temporal resolution. Using this model, we aim to investigate the influence of environmental variables on vertical strategies, and how vertical strategies affect fitness and phenology in seasonal environments. We further discuss how short-term behavior (DVM) influences and interacts in the longer-term and shape-up different life history components of copepod strategies.

2. Materials and methods

Although the model is not strictly individual-based, it is described following the Overview, Design concepts and Details (ODD) protocol (Grimm et al., 2006, 2010) to improve reproducibility.

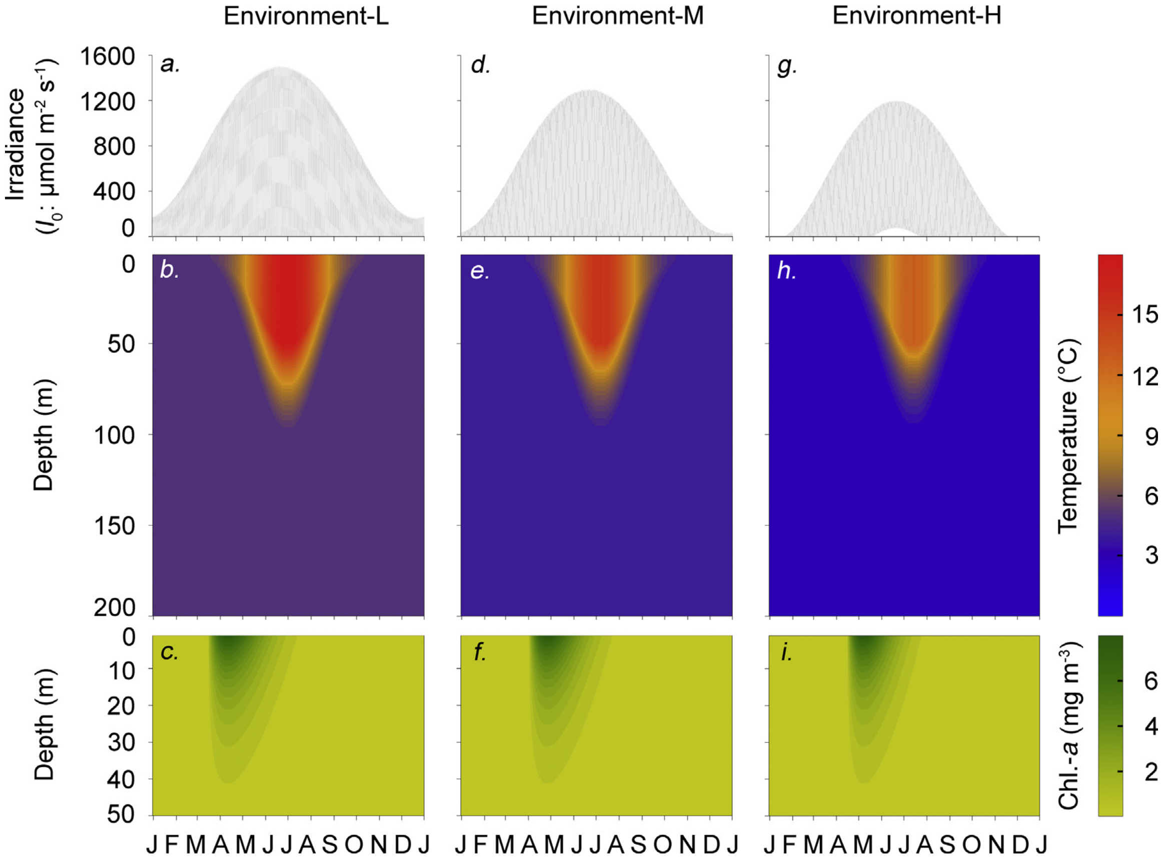

Fig. 1. The modelled dynamics of irradiance incident on the sea surface (hourly estimates; a, d, g), temperature (b, e, h) and food availability (c, f, i, expressed as Chlorophyll-*a* biomass) in the three model environments. See Appendix A1 in Supplementary material for a detailed comparison.

2.1. Purpose

The purpose of the model is to investigate the bottom-up and top-down influences of environmental variability (i.e. irradiance, temperature, food-availability and predation risk) on vertical strategies of a high-latitude herbivorous copepod, and to understand the influences of vertical strategies on its fitness and phenology.

2.2. Entities, state variables and scales

The model consists of three entities: vertical strategies, model organism and the model environment. Vertical strategies define the timing, amplitude and the ontogenetic trajectories of DVM and SVM, and are described using six evolvable (soft) parameters (Table 2). These are hardwired to the model organism, i.e. copepods spawned in different times of the year.

The model organism is a hypothetical herbivorous semelparous female copepod (hereafter, the copepod) with an annual life cycle that resembles *Calanus finmarchicus* and *C. glacialis* in terms of body size, behavior and life history strategies (Conover, 1988). These two species often dominate the copepod biomass in the North Atlantic and most Eurasian sub-Arctic and Arctic seas and shelves (Falk-Petersen et al., 2009). Their life cycle consists of an embryonic stage (egg), six naupliar stages (NI–NVI), five copepodite stages (CI–CV) and an adult. Eggs that are released in near-surface waters in the spring usually develop into CIV or CV stages toward the end of the productive season. As further development is typically constrained by the duration of the productive season and seasonal peaks of visual predation risk, CIVs and CVs descend into deeper waters and remain in a state of diapause/dormancy with minimal physiological activity (Hirche, 1996). Overwintering stages ascend to near-surface waters as the primary production commences in the following year, molt into adults and start to reproduce (Conover, 1988; Varpe, 2012). The life cycle of the two species is usually completed within one year in most sub-Arctic and Arctic locations (Falk-Petersen et al., 2009; Daase et al., 2013), within which reside the model environments of this study.

The model runs in three 500-m deep artificial seasonal environments that represent three high-latitude locations along the southern and southeastern coast of Norway (60–70°N). These environments do not point to specific geographic locations, but the modelled environmental dynamics were adopted from field measurements from the above region (Appendix A1 in Supplementary material). The baseline model simulation (hereafter, the basic run) runs in Environment-L, representing the lower end (ca. 60°N) of the selected geographical range. Here, the modelled irradiance, temperature and food availability are highly seasonal and vertically structured (Fig. 1a–c), but are assumed constant between years. The irradiance incident on the sea surface follows the global clear-sky horizontal irradiance model of Robledo and Soler (2000), and peaks at ca. 1500 µmol m^{-2} s^{-1} (Fig. 1a, Appendix A1 in Supplementary material). The sea surface temperature reaches a maximum of 18 °C in the summer (e.g. Bagøien et al., 2000), and distributes evenly in the surface mixed layer (Fig. 1b). Below this, the temperature decreases with depth and converges to a minimum of 4 °C at ca. 100 m (e.g. Ingvaldsen and Loeng, 2009). The pelagic productive season extends ca. 180 days, with a chlorophyll-*a* peak at 8 mg m^{-3} in mid-April (Fig. 1c: Sakshaug et al., 2009; Daase et al., 2013). We manipulated the environmental parameters of Environment-L to formulate two additional artificial environments: Environment-M (ca. 65°N, Fig. 1d–f) and Environment-H (ca. 70°N, Fig. 1g–i),

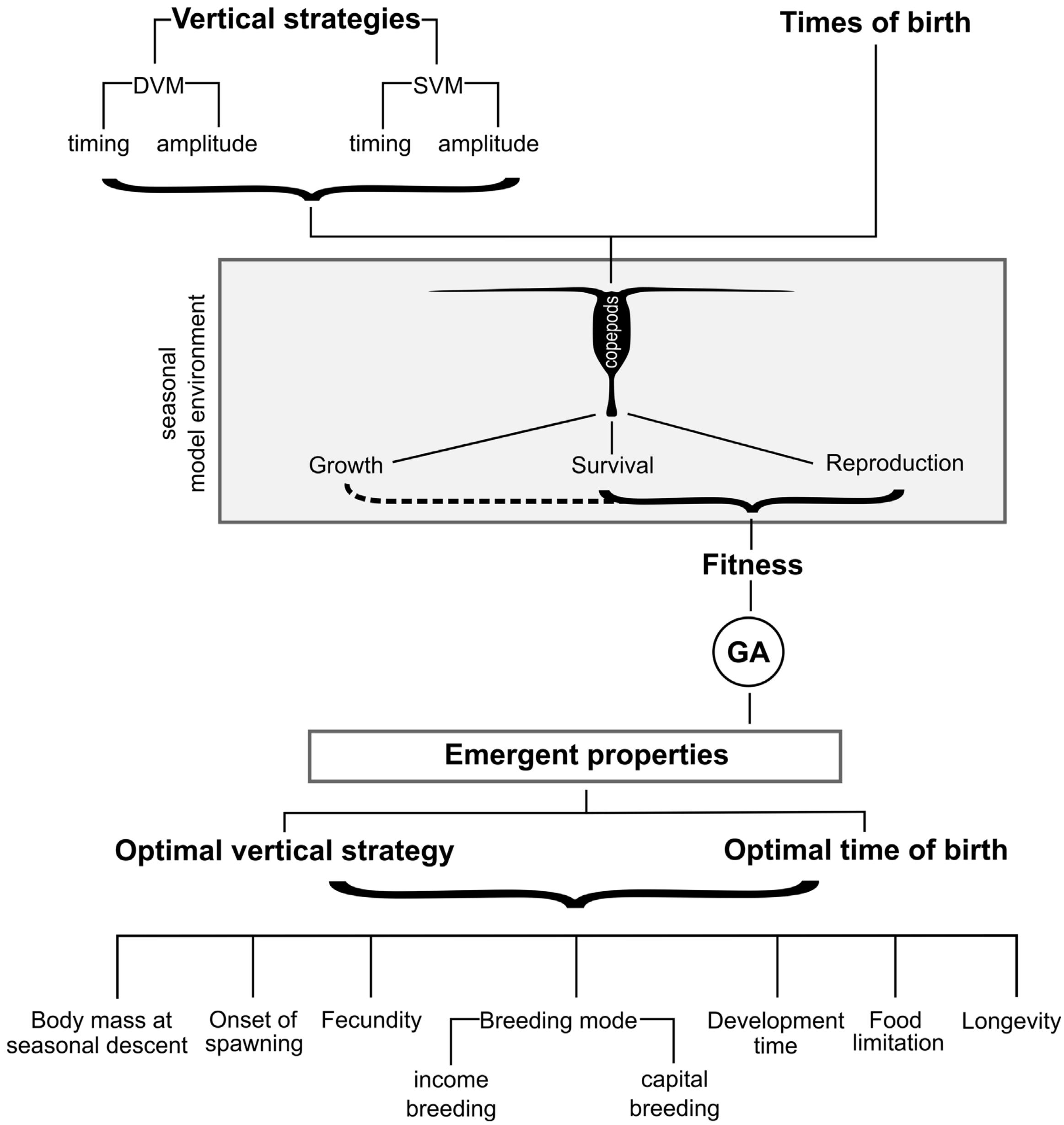

Fig. 2. The model overview. Vertical strategies that define the timing and amplitude of DVM and SVM are hardwired to copepods born in different times of the year. Growth, survival and reproduction of these copepods are simulated in a seasonal environment to derive a fitness estimate that is heuristically maximized by the GA to derive the optimal vertical strategy, time of birth and several associated life history traits emerging from the model. Dashed line represents the indirect dependency of the fitness estimate on growth (Section 2.6.4).

representing the mid-point and the higher end of the selected geographical range (Appendix A1 in Supplementary material).

Copepods are characterized by six states: vertical location (depth), structural body mass, energetic reserve, reproductive output (fecundity), survivorship and developmental stage. The model has a temporal coverage of an annual cycle and a unidimensional (vertical) spatial coverage of 500 m. The time and space consist of 1 h and 1 m discreet intervals.

2.3. Process overview and scheduling

At each timestep, the model follows vertical strategies hardwired to copepods born in different times of the year and simulates their growth, survival and reproduction. State variables are updated simultaneously. Vertical strategies are evaluated using a fitness function based on the expected survival and reproductive performances. The fitness is heuristically maximized using a Genetic Algorithm (GA, Holland, 1975) to estimate the optimal vertical strategy and optimal time of birth for a given set of environmental conditions (Fig. 2).

2.4. Design concepts

2.4.1. Basic principles

The high spatial and temporal resolution implemented in the model allow both DVM and SVM to be simulated over the entire annual life cycle of the copepod. Carlotti and Wolf (1998) have implemented a similar construct, but the SVM of their model was constrained by fixing the timing of ascent and descent to match the field observations of the region of interest. In contrast, the timing and the amplitude of DVM and SVM of our model are flexible and allowed to evolve according to the environmental conditions. To

Table 3
Emergent properties of the model. The timing and amplitude and of DVM and SVM altogether forms the vertical strategy of a copepod.

Trait/attribute	Units	Description
Time of birth	Day of the year	Time of being spawned
Surface time	h	Unified estimate representing the timing of DVM, i.e. the stage-specific mean no. of hours per day occupied in waters with highest growth potential (usually the surface waters)
Amplitude of diel vertical migration	m	The vertical range corresponding to the above
Time of seasonal descent and ascent	Day of the year	Separate estimates representing the timing of SVM (ascent and descent)
Amplitude of seasonal vertical migration	m	Overwintering depth
Body mass at seasonal descent	μg C	Structural and energetic reserve mass at the onset of diapause
Onset of egg production	Day of the year	–
Fecundity	No. of eggs	No. of eggs produced during the lifetime
Breeding mode index	dim.less	Proportion of capital breeding eggs (0 = pure income breeding, 1 = pure capital breeding)
Food limitation index	dim.less	Stage-specific total no. hours with food-limited growth (Eq. (3)) as a fraction of stage duration (0 = no food limitation, 1 = total food limitation)
Development time	d	From egg to a given stage
Longevity	d	Duration of the life cycle, from birth to death

achieve this level of flexibility, we used multiple evolvable proxies to represent vertical migration (Table 2). This resulted in a complex seven-dimensional optimization problem that can be efficiently solved using heuristic techniques (Zanakis and Evans, 1981). As evolutionary algorithms provide an efficient means of solving multi-dimensional optimization problems (Deb, 2001; Eiben and Smith, 2003), we used a GA as the optimization platform of this model. Further, to increase the precision of the evolvable parameters and that of the behavioral strategies and life history traits ensued (Fig. 2), we used a GA variant with floating point representation (i.e. a Real-Coded Genetic Algorithm, Davis, 1989; Lucasius and Kateman, 1989; Herrera et al., 1998).

The strategy-oriented construct of this model contrasts classic individual-based models of zooplankton life history and behavior in two main ways: first, trading off of biological resolution (strategies vs. individuals) to accommodate higher spatio-temporal resolution, and second, the lack of population-level responses such as density dependence. As a result, modelled vertical strategies do not interact with each other and show no quantitative feedbacks with the model environment (e.g. impact of grazing on food concentration and duration of the productive season).

2.4.2. Emergence

The behavioral strategies and life history traits emerging from the model are presented in Fig. 2 and described in Table 3.

2.4.3. Adaptation and sensing

Copepods are sensitive to their internal states (i.e. structural body mass, mass of the energetic reserve and developmental stage) and external stimuli (i.e. irradiance, temperature, food concentration and depth). Altogether, these determine the size- or stage-specific patterns of growth, metabolism, reproduction and vertical behavior (Section 2.6).

2.4.4. Objectives

The model uses a fitness estimate that evaluates the expected reproduction and survival performances rendered by different vertical strategies (Section 2.6.4).

2.4.5. Prediction and stochasticity

The vertical search pattern of copepod behavior is based on a semi-stochastic predictive algorithm (Section 2.6.2.2 and Appendix A2 in Supplementary material). Stochasticity plays a central role in the model initialization (Section 2.5) and selection, recombination and mutation operators of the GA (Section 2.6.4).

2.4.6. Observations

For a given model environment, the model produces heuristic estimates of the optimal vertical strategy and optimal time of birth, along with a range of associated life history traits (Fig. 2, Table 3).

2.5. Initialization

The model initializes with seeding of N (=10^6) eggs at random times of the year to random depths (<50 m) of the water column. Each seed represents an embryonic stage of a copepod with a specific vertical strategy, which is determined by randomly assigning values to the evolvable proxies. The ranges (bounds) and resolutions of these proxies are listed in Table 2.

2.6. Submodels

2.6.1. Growth and development

We modelled somatic growth in Carbon units (μg C) according to the growth model of Huntley and Boyd (1984) (Eqs. (1)–(8) below), using a Chlorophyll-a/C ratio of 0.030 (Båmstedt et al., 1991; Sakshaug et al., 2009). This growth sub-model was used due to its simplicity and general applicability, which are shown by its utility to model several different copepod taxa with varying body sizes representing a wide range of geographical locations (e.g. Robinson, 1994; Fiksen and Giske, 1995; Roman et al., 2000). Definitions and units of all the terms described henceforth are listed in Table 4.

For ambient food concentrations (F: μg C ml^{-1}) above a specific saturation concentration (f), growth is food-independent, and occurs at a maximum rate (G_T: μg C ind^{-1} h^{-1}) dependent only on the ambient temperature (T) as;

$$(G_T)_{i,t,z} = \left(G'_{max}\right)_{t,z} \cdot W_{i,t} \tag{1}$$

Here, i represents individual, t time and z is depth, where $G'_{\max}$ (μg C mg dry mass h^{-1}) is the maximum temperature-dependent mass-specific growth rate, assuming a Carbon: dry body mass (W, mg) ratio of 0.40 (Huntley and Boyd, 1984), defined as;

$$\left(G'_{\max}\right)_{t,z} = 0.903 \cdot \exp\left(0.110 \cdot T_{t,z}\right) \tag{2}$$

If the ambient food concentration drops below the saturation concentration, the growth occurs at a rate limited by food availability (G_F) as;

$$(G_F)_{i,t,z} = a \cdot b_{t,z} \cdot W_{i,t}^{n_{t,z}} \cdot F_{t,z} - k \cdot W_{i,t}^{m_{t,z}} \tag{3}$$

Table 4
Definitions, values and units of the terms used in the model.

Term	Definition	Value/formula	Units
a	Assimilation coefficient	0.70[b]	–
$b_{t,z}$	Clearance coefficient	Eq. (4)[a]	ml mg dry mass h^{-1}
E	Egg development parameter	717[e,f]	–
$f_{i,t,z}$	Saturation food concentration	Eq. (8)[a]	µg C ml^{-1}
$F_{t,z}$	Ambient food concentration	Section 2.2	µg C ml^{-1}
$(G'_{max})_{t,z}$	Maximum mass-specific growth rate	Eq. (2)[a]	µg C mg dry mass h^{-1}
$(G_F)_{i,t,z}$	Food-limited growth rate	Eq. (3)[a]	µg C ind^{-1} h^{-1}
$(G_T)_{i,t,z}$	Non food-limited growth rate	Eq. (1)[a]	µg C ind^{-1} h^{-1}
$H_{i,t,z}$	Survivorship	Eq. (15)	–
i	Individual	–	–
$I'_{t,z}$	Remapped $I_{t,z}$	$0.9 \geq I' \geq 0.1$	–
$I_{t,0}$	Irradiance incident on sea surface	Appendix A1 in Supplementary material[c]	µmol m^{-2} s^{-1}
$I_{t,z}$	Downwelling irradiance at depth z	Eq. (9)	µmol m^{-2} s^{-1}
j	Developmental stage	0–12 (Egg–Adult)	–
$K_{i,t}$	Scalar for visual predation risk	$1 > K > 0$	–
$k_{t,z}$	Respiratory coefficient	Eq. (5)[a]	µg C mg dry mass h^{-1}
$(M_n)_{t,z}$	Non-visual predation risk	Section 2.6.2.1	–
$(M_s)_{i,t,z}$	Starvation risk	Eq. (12)	–
$m_{t,z}$	Exponent (respiration)	Eq. (6)[a]	–
$(M_v)_{i,t,z}$	Visual predation risk	Eq. (10)	–
N	No. of initial seeds	1,000,000	–
$n_{t,z}$	Exponent (clearance)	Eq. (7)[a]	–
R_i	Fecundity	Eq. (13)	no. of eggs
t	Time	1–8760	h
$T_{t,z}$	Ambient temperature	Section 2.2	°C
$U_{i,t}$	Cruising velocity	Eq. (11)	m h^{-1}
$(W_c)_{i,t}$	Structural mass	–	µg C
W_E	Unit egg mass	0.55[d]	µg C
$W_{i,t}$	Dry body mass (assuming 40% C)	–	mg
$(W_q)_{i,t}$	Catabolized structural mass (proportion to the maximum lifetime structural mass)	$0 \geq W_q \geq 0.5$	–
$(W_R)_{i,t,z}$	Matter allocated for egg production	–	µg C
$(W_s)_{i,t}$	Storage (energetic reserve) mass	–	µg C
W_x	Stage-specific critical molting mass	Table 5	µg C
z	Depth	0–500	m
Φ	Termination condition of the RCGA	Section 2.6.4	–
ψ	Light attenuation coefficient	0.06[g]	m^{-1}
ω	Parameter for weighing fitness	0 or 1	–
Ω_i	Fitness	Eq. (14)	–

[a] Huntley and Boyd (1984).
[b] Fiksen and Giske (1995).
[c] Robledo and Soler (2000).
[d] Calculated from Salzen (1956).
[e] Campbell et al. (2001).
[f] Ji et al. (2012).
[g] Eiane and Parisi (2001).

where two terms of the right-hand side of the equation refer to the assimilation and respiratory rates respectively. The assimilation coefficient (a) is assumed to be constant (Table 4), but Huntley and Boyd (1984) found that the coefficients of clearance (b) and respiration (k), and the exponents (n and m) vary with ambient temperature as;

$$b_{t,z} = 1.777 \cdot \exp(0.234 \cdot T_{t,z}) \tag{4}$$

$$k_{t,z} = 0.375 \cdot \exp(0.0546 \cdot T_{t,z}) \tag{5}$$

$$n_{t,z} = 0.671 \cdot \exp(0.0199 \cdot T_{t,z}) \tag{6}$$

$$m_{t,z} = 0.858 \cdot \exp(-0.008 \cdot T_{t,z}) \tag{7}$$

At the point where F reaches f, Eqs. (1) and (3) balance out, and the f becomes;

$$f_{i,t,z} = \frac{\left[\left(G'_{max}\right)_{t,z} \cdot W_{i,t} + k_{t,z} \cdot W_{i,t}^{m_{t,z}}\right]}{a \cdot b_{t,z} \cdot W_{i,t}^{n_{t,z}}} \tag{8}$$

This growth sub-model is not applicable to the first two nauplii stages, which do not feed (Fig. 3a, Marshall and Orr, 1972; Mauchline, 1998). For simplicity, we assumed the growth of NI and NII stages to occur at a temperature-dependent rate (Eqs. (1) and (2)). The growth of early developmental stages (NI–CIII) is solely allocated to the building up of structural mass (W_c, µg C, Fig. 3a, b and Table 5).

The embryonic development follows a Bělehrádek temperature function (Campbell et al., 2001; Ji et al., 2012). The post-embryonic development (from stage j to $j+1$) occurs only if W_c exceeds a stage-specific critical molting mass (W_x, µg C, Table 5). However, for simplicity, we did not model the dependence of molting process on the physiological state (Nival et al., 1988) and the limitation of growth by the exoskeleton (Mauchline, 1998).

2.6.2. Survival

2.6.2.1. Predation risk. Visual (v) and non-visual (n) predators induce mortality, which is estimated as a probability following Eiane and Parisi (2001) as;

$$I_{t,z} = I_{t,0} \cdot \exp\left(-\psi \cdot z\right) \tag{9}$$

where I_z and I_0 are irradiance at depth z and surface at a given time, and ψ (=0.06 m^{-1}) is the attenuation coefficient for downwards directed irradiance in the water column. We remapped irradiance (I) between 0.1–0.9 (I') so that visual predation risk is not nullified even at the lowest levels of irradiance, and the copepod has some chance of survival even at highest levels of irradiance.

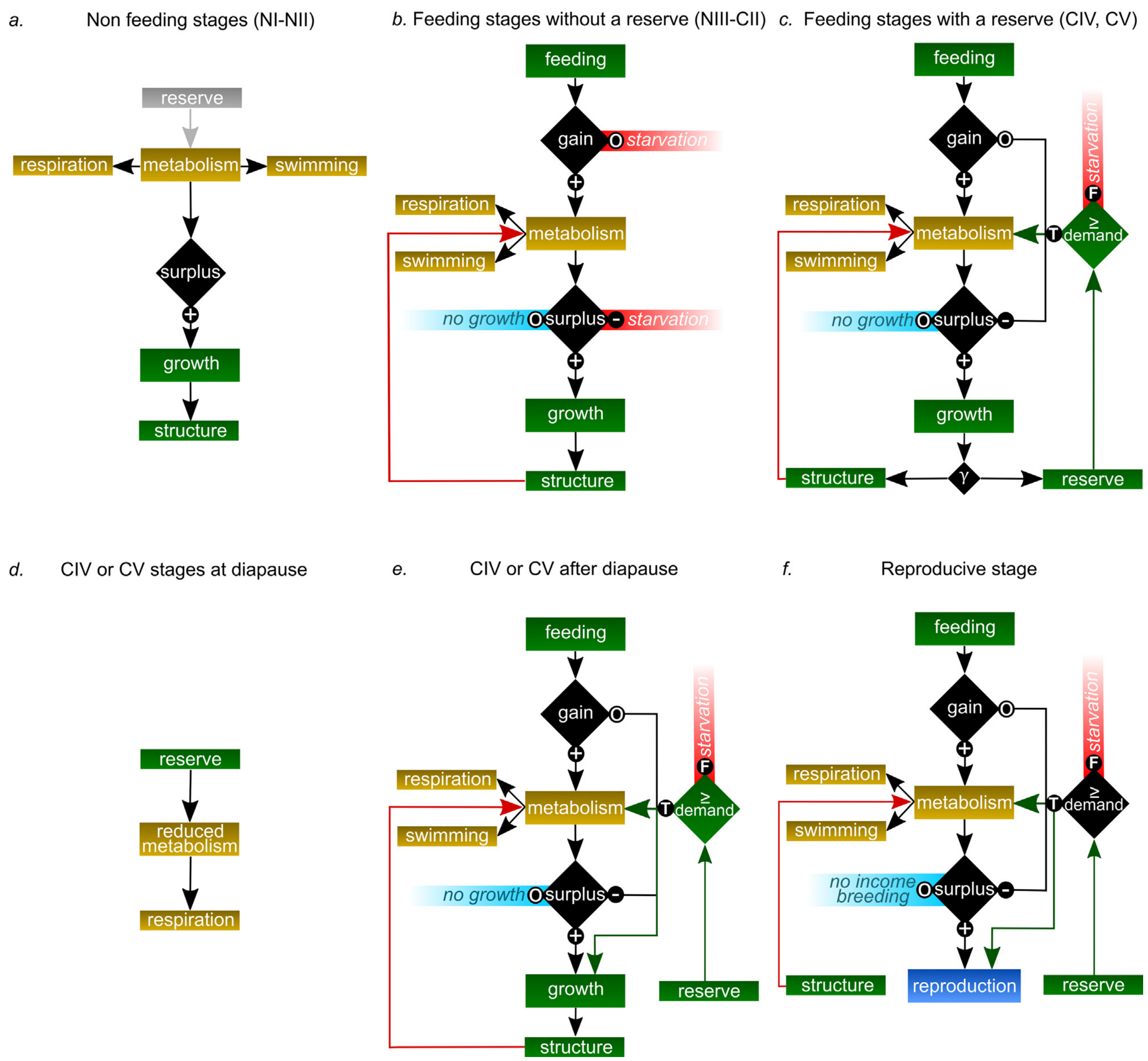

Fig. 3. Simplified physiological pathways modelled in this study. Some life stages are grouped together due to their similarities in energy allocation patterns (a–f). Starvation (highlighted in red) triggers catabolic pathways marked in red. T and F are Boolean values true and false. γ is the growth allocation parameter (Table 2). A comparative summary is given in Table 5.

The detection efficiency of visually orientating planktivores increases with the size of their prey (Brooks and Dodson, 1965; Batty et al., 1990). For simplicity, we modelled the size-dependent visual predation risk using a linear model, assuming that the largest developmental stage is ca. 10 times more vulnerable to visual predators compared to the smallest developmental stage (Fig. 4a, Table 5, De Robertis, 2002). This was implemented using the scalar K ($1 > K > 0$) as;

$$(M_v)_{i,t,z} = I'_{t,z} \cdot K_{i,t} \tag{10}$$

The initial value of K (i.e. K value at the embryonic stage, range = 1×10^{-4}–1.5×10^{-2}) was decided so that it produces hourly estimates of visual predator-induced mortality.

We assumed the mortality risk caused by non-visual predators (non-visual predation risk, M_n) to be 1% of the maximum visual predation risk and constant over time and depth (Eiane and Parisi, 2001).

2.6.2.2. Diel vertical migration. The copepod may perform DVM to trade off growth potential to minimize the visual predation risk. We used the photoreactive behavior as a proxy to estimate the timing and amplitude of DVM (e.g. Kerfoot, 1970; Carlotti and Wolf, 1998). Here, α, an evolvable light sensitivity parameter (Table 2) was used to define an irradiance threshold above which induces a negative phototatic response in the vertical swimming behavior (Båtnes et al., 2015; Cohen et al., 2015). At any given time, the copepod occupies a depth with an irradiance level ($I_{t,z}$) below α. From a series of possible depth bins that satisfy the $I_{t,z} < \alpha$ condition, we assumed that the copepod searches and occupies the depth that maximizes its growth potential. For simplicity, we further assumed that internal state-dependent factors, such as hunger and satiation have a negligible influence on the modelled DVM. The vertical search pattern was predicted using a biased random walk algorithm (Codling, 2003, Appendix A2 in Supplementary material), assuming that the copepod is neutrally buoyant and vertically moves in the water column at a maximum velocity (hereafter cruising veloc-

Table 5
Developmental stages, their maximum structural body masses (W_x) and stage-specific variability in several biological processes modelled in this study (cf. Fig. 3). Dashes indicate non-applicability.

Stage	W_x (μgC)	Feeding	Structural growth	Energetic Reserve	Respiration	Swimming	Egg production
Egg	0.55	–	–	–	–	–	–
NI	0.55	–	x	–	x	x	–
NII	0.68	–	x	–	x	x	–
NIII	0.91	x	x	–	x	x	–
NIV	1.84	x	x	–	x	x	–
NV	2.72	x	x	–	x	x	–
NVI	3.92	x	x	–	x	x	–
CI	6.01	x	x	–	x	x	–
CII	9.84	x	x	–	x	x	–
CIII	17.58	x	x	–	x	x	–
CIV	36.42	x[a]	x[d]	x	x[c]	x[d]	–
CV	110.03	x[a]	x[d]	x	x[c]	x[d]	–
Adult	332.27	x	–	x[b]	x	x	x

W_x values resemble those published for *C. finmarchicus* and *C. glacialis* by Båmstedt et al. (1991); and Campbell et al. (2001).

[a] Feeding ceases during diapause.

[b] Does not allocate surplus growth to develop the energetic reserve, but inherit the reserves from its developmental progression.

[c] Reduces during diapause.

[d] Not relevant during diapause.

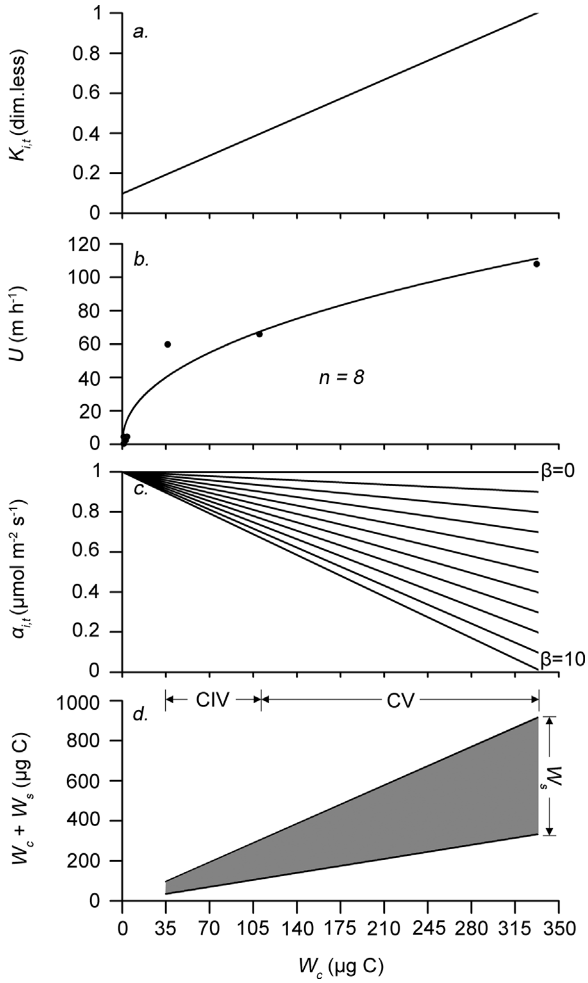

Fig. 4. Relationships of (a) visual predation risk scalar, (b) cruising velocity, (c) light sensitivity parameter and (d) the total body mass of the copepod with its structural mass (W_c). The cruising velocity (U) model was fitted using laboratory and field estimates of *Calanus* spp. from Hardy and Bainbridge (1954), Greene and Landry (1985) and Heywood (1996) (points in panel b). The different linear models for β, that scale the light sensitivity parameter (α) are optimized in the model (Table 2). The lower and upper border of the shaded polygon (panel d) represent the total body mass for growth allocation parameter (γ) = 0 and 1 respectively.

ity, U). We used several stage-specific cruising velocity estimates of *Calanus* spp. available in the literature (Fig. 4b), and related those to body mass as;

$$U_{i,t} = 8.0116 \cdot (W_c)_{i,t}^{0.4531} \qquad (11)$$

We considered the size- or stage-specific variability of DVM as a response to size-dependent visual predation risk (Zaret and Kerfoot, 1975; Uye et al., 1990; Hays et al., 1994; Eiane and Ohman, 2004) and modelled it by scaling the light sensitivity parameter (α) with the body mass (W_c). As data on the light sensitivity of younger developmental stages (NI–CIII) of *Calanus* spp. is rare, we could not derive a general relationship between W_c and α. To address this, we defined an evolvable parameter β that describes the size specificity of α, which, at its maximum ($\beta = 10$) downscales α of the adult female to 10% of that of the egg/NI (Fig. 4c). Higher trajectories than $\beta = 10$ were not used, as it was shown in the trial runs that the model always converges on $\beta < 10$ even at highest levels of visual predation risk.

2.6.2.3. *Energy storage.* CIV and CV stages can allocate a specific fraction from surplus growth (evolvable growth allocation parameter: γ, Table 2) to build up an energy reserve (Fig. 3c) that possesses a maximum size of 70% of the total body mass (Fig. 4d, Fiksen and Carlotti, 1998).

2.6.2.4. *Seasonal vertical migration.* Similar to most high-latitude marine zooplankton, which descend to depths during the unproductive part of the year (reviewed in Conover, 1988; Hagen and Auel, 2001; Falk-Petersen et al., 2009), the copepod may perform SVM. We used the state of the energetic reserve as a proxy of timing of the SVM (cf. Visser and Jónasdóttir, 1999). Here, the copepod descends to a specific depth (evolvable overwintering depth ζ, Table 2) when the stores account for a specific fraction of the total body mass (evolvable seasonal descent parameter: δ, Table 2). Upon reaching the overwintering depth, the copepod remains stagnant at a diapause state (Hirche, 1996) with its metabolic rate reduced by 90% from that under normal conditions (Fig. 3d, Table 5, Pasternak et al., 1994; Varpe et al., 2007). The overwintering period terminates when a specific fraction (evolvable seasonal ascent parameter: ε, Table 2) of the energetic reserve is exhausted. After the overwintering period, surplus gains are not allocated to develop further energetic reserves, but may be used for structural growth and reproduction (Fig. 3e and f, Table 5).

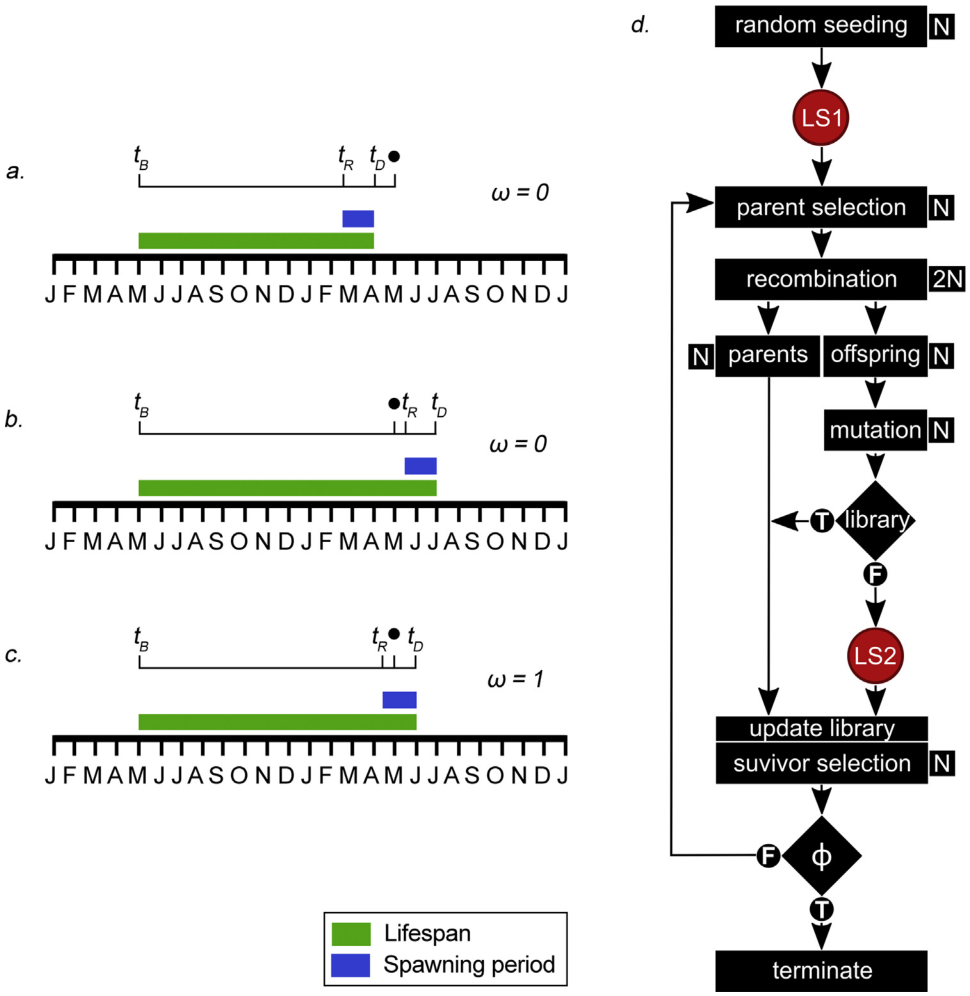

Fig. 5. (a–c) Mechanism of weighing fitness. Fitness of a copepod is multiplied by a binary weight ω = 0 if its egg production season ($t_D - t_R$) does not overlap the time of birth (t_B, May 1 in this example, denoted by a black dot) and vice versa. (d) Simplified workflow of initialization and optimization steps of the model. The initial set of strategies enter the optimization loop after going through the first life cycle simulation (LS1). The GA optimizes seven evolvable (soft) parameters (Table 2) by repeatedly applying selection, recombination and mutation operators until a termination condition (φ) is satisfied. T and F are Boolean true and false conditions. No. of strategies (i.e. size of the GA-population, N or $2N$) at each operation is indicated to the right.

2.6.2.5. Metabolism. The basal metabolic cost relates with the body mass and ambient temperature, expressed as $k{\cdot}W^m$ in Eq. (3) (terms as defined above and in Table 4). The metabolic cost of zooplankton vertical movements can account for 0–300% of the basal metabolic demand (Vlymen, 1970; Foulds and Roff, 1976; Morris et al., 1985; Dawidowicz and Loose, 1992). For simplicity, we assumed the cost of vertical movement to be 150% of the basal metabolic cost (mid-point of the above range). This additional cost is subtracted from the growth Eqs. (1) or (3). The energy reserve is used to balance the metabolic demands that cannot be sustained under low ambient food concentrations (Fig. 3c–f).

2.6.2.6. Starvation risk. When energy reserves are depleted, the metabolic demands that cannot be balanced by food intake are met by catabolizing structural body mass (Fig. 3b–f). This elevates the mortality risk due to starvation (starvation risk, M_s), which is defined as a probability that increases as a linear function of catabolized structural mass as;

$$(M_s)_{i,t} = 2 \cdot \left(W_q\right)_{i,t} \qquad (12)$$

Here, W_q is the catabolized structural mass expressed as a proportion of the maximum structural mass prior to structural catabolization. W_q can reach a maximum of 0.5, during which M_s peaks following Eq. (12), and the copepod dies according the Chossat's rule (Chossat, 1843), which posits that starving animals may catabolize about half of their body weight before death. Irrespective of the age of this generalized rule, it has been used as a constraint in starvation studies of many vertebrate and invertebrate taxa (e.g. Threlkeld, 1976; Spencer, 1997; Costello, 1998; Loos et al., 2010).

2.6.3. Reproduction

We assumed that somatic growth ceases after the final molt, and all adults become sexually mature at a constant structural body mass (Fig. 3f, Table 5). Energetic input to egg production may be sourced from food intake (income breeding) or allocating a specific amount of matter (C) equivalent to the maximum growth rate (G_T: Eqs. (1) and (2)) from the remaining energetic reserve (capital breeding, cf. Varpe et al., 2009). The fecundity (R) from the time of sexual maturity (t_R = time of final molt) to a given time horizon (t_X) is estimated using the matter allocated to egg production (W_R) and the unit egg mass (W_E = 0.55 µg C) as;

$$R_i = \sum_{t_R}^{t_X} \frac{(W_R)_{i,t,z}}{W_E} \qquad (13)$$

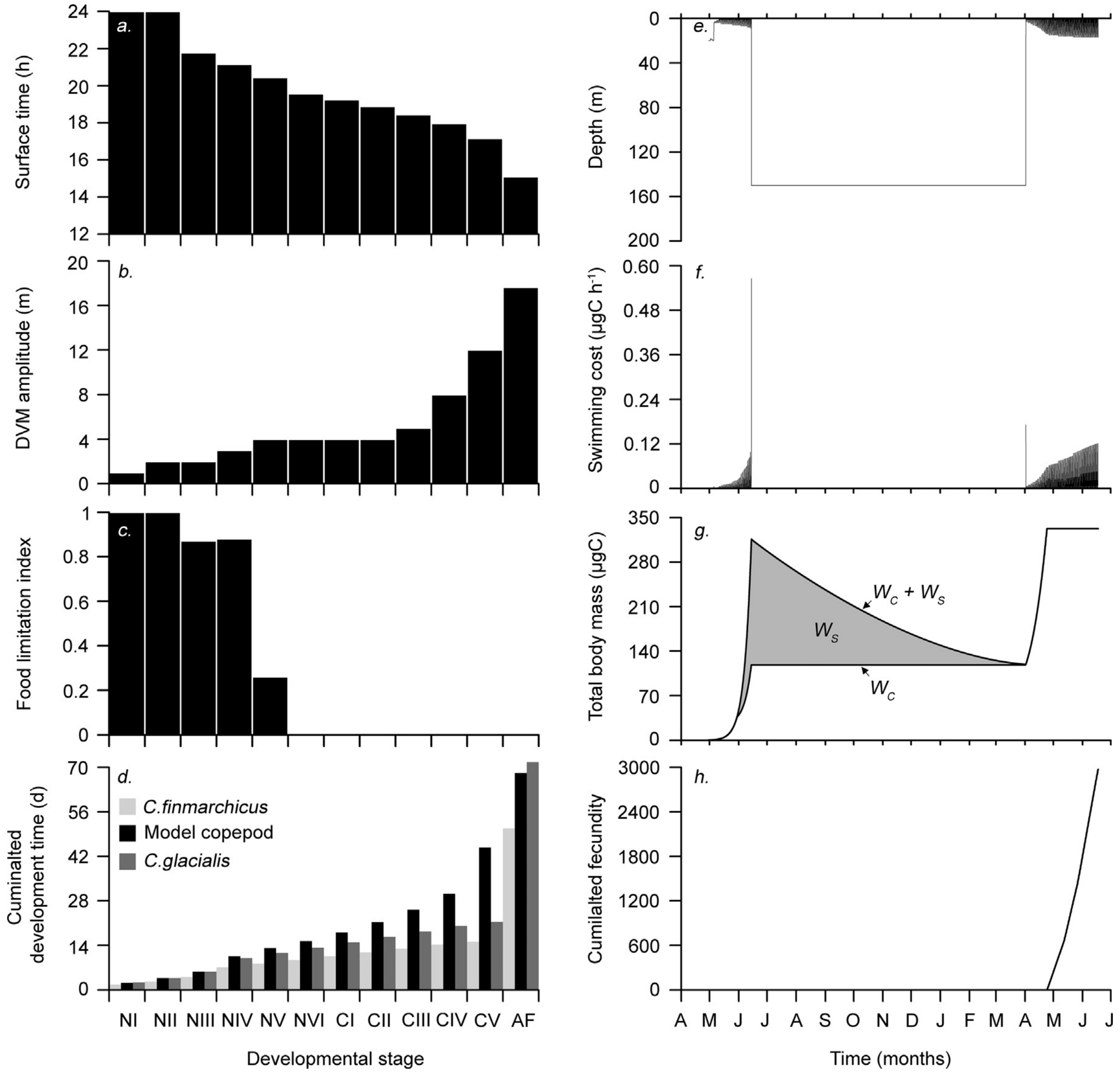

Fig. 6. Predicted optimal vertical strategy and associated growth and reproductive performances of the copepod in the basic run at Environment-L (cf. Fig. 1a–c). The surface time (a) is the stage-specific mean no. of hours per day that the copepod occupies food-rich surface waters, and amplitude (b) is its vertical range. Panel d compares predicted development times (excluding overwintering duration) to those estimated for *C. finmarchicus* and *C. glacialis* following Bělehrádek functions parameterized by Campbell et al. (2001) and Ji et al. (2012). W_c and W_s refer to structural body mass and size of the energetic reserve respectively.

2.6.4. *Fitness function and optimization*

To evaluate the performance of a vertical strategy, we derived a fitness estimate (Ω) as a function of survivorship and fecundity as;

$$\Omega_i = \left(\sum_{t_B}^{t_X} H_{i,t,z} \cdot R_{i,t,z} \right) \cdot \omega \tag{14}$$

Here, ω is a weight that adjusts fitness (see below) and H is the survivorship, i.e. the probability of survival from birth (t_B) to a given time horizon (t_X) estimated as a function of visual, non-visual and starvation risks (M_v, M_n and M_s) as;

$$H_{i,t,z} = \prod_{t_B}^{t_X} 1 - \left[(M_v)_{i,t,z} + (M_n)_{t,z} + (M_s)_{i,t} \right] \tag{15}$$

The term Ω technically resembles the net reproductive rate (e.g. Stearns, 1992), and is used in some optimization models (e.g. Kiørboe and Hirst, 2008) but may not bare the same interpretation given the strategy-oriented construct of this model. When the model predicts an optimal vertical strategy and time of birth for a particular environment, we can assume that those predicted optima should persist from one generation to the next if the environment remains constant. If a copepod's spawning period lasts from time t_R to t_D (time of death) we assumed that it produces a series of offspring with the same vertical strategy, but born at different times of the year (ranging from t_R to t_D). However, only the offspring with a time of birth matching that of the mother can represent the entire evolvable (soft) parameter set of the mother, and guarantee its persistence from one generation to another (Fig. 5a–c). Therefore, we adjusted the fitness using a binary weight (ω) by setting $\omega = 0$ if the copepod's spawning season does not overlap its time of birth (Fig. 5a and b) and vice versa (Fig. 5c).

We used a Real-Coded Genetic Algorithm (RCGA) to derive heuristic estimates of optimal vertical strategy and time of birth that maximizes fitness in a given model environment (Fig. 5d). In the RCGA, six proxies of vertical strategies and the time of birth of the copepod that those are hardwired to (Table 2) are considered as genes on a single chromosome. The RCGA begins by selecting a mating pool of N chromosomes (=parents, i.e. N vertical strategies seeded in different times of the year) from the initial

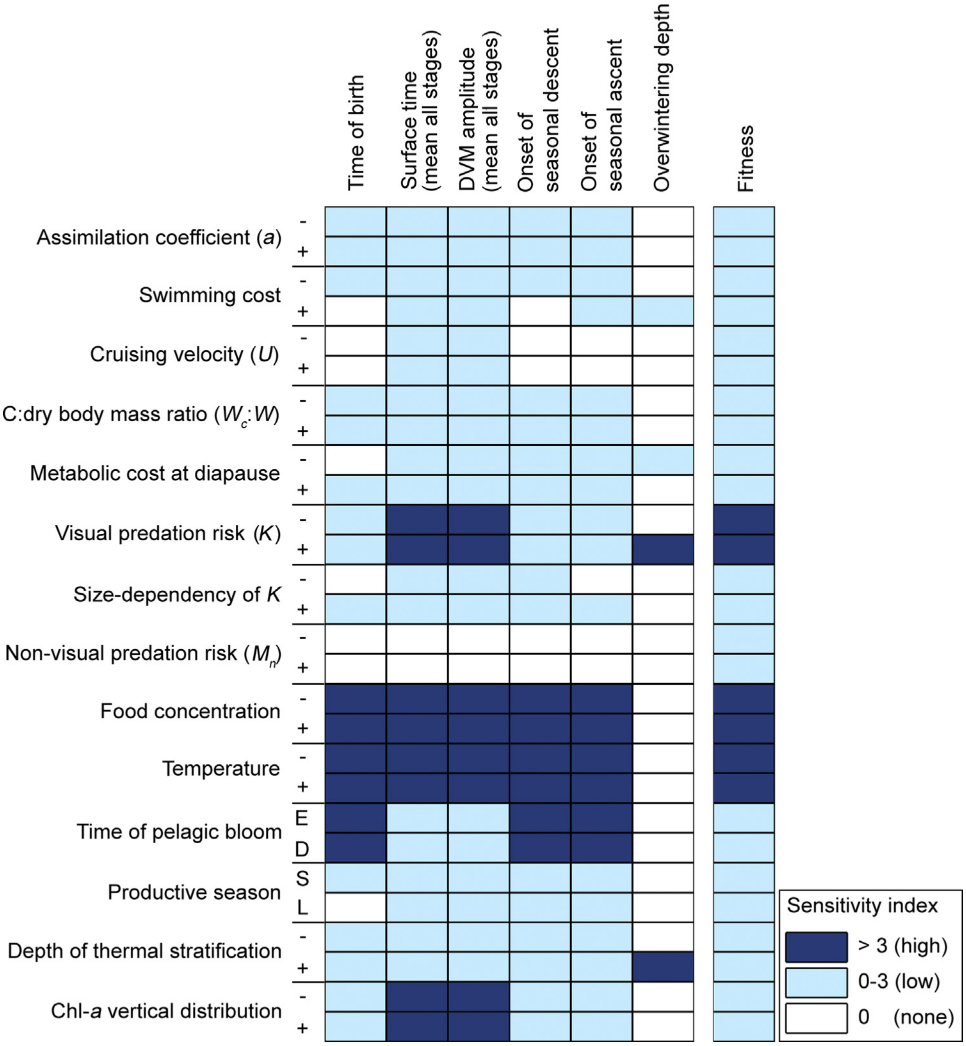

		Time of birth	Surface time (mean all stages)	DVM amplitude (mean all stages)	Onset of seasonal descent	Onset of seasonal ascent	Overwintering depth	Fitness
Assimilation coefficient (*a*)	-	▨	▨	▨	▨	▨	□	▨
	+	▨	▨	▨	▨	▨	□	▨
Swimming cost	-	▨	▨	▨	▨	▨	□	▨
	+	□	▨	▨	□	▨	▨	▨
Cruising velocity (*U*)	-	□	▨	▨	□	□	□	▨
	+	□	▨	▨	□	□	□	▨
C:dry body mass ratio (W_c:*W*)	-	▨	▨	▨	▨	▨	□	▨
	+	▨	▨	▨	▨	▨	□	▨
Metabolic cost at diapause	-	□	▨	▨	▨	▨	□	▨
	+	▨	▨	▨	▨	▨	□	▨
Visual predation risk (*K*)	-	▨	■	■	▨	▨	□	■
	+	▨	■	■	▨	▨	■	■
Size-dependency of *K*	-	□	▨	▨	▨	□	□	▨
	+	▨	▨	▨	▨	▨	□	▨
Non-visual predation risk (M_n)	-	□	□	□	□	□	□	▨
	+	□	□	□	□	□	□	▨
Food concentration	-	■	■	■	■	■	□	■
	+	■	■	■	■	■	□	■
Temperature	-	■	■	■	■	■	□	■
	+	■	■	■	■	■	□	■
Time of pelagic bloom	E	■	▨	▨	■	■	□	▨
	D	■	▨	▨	■	■	□	▨
Productive season	S	▨	▨	▨	▨	▨	□	▨
	L	□	▨	▨	▨	▨	□	▨
Depth of thermal stratification	-	▨	▨	▨	▨	▨	□	▨
	+	▨	▨	▨	▨	▨	■	▨
Chl-*a* vertical distribution	-	▨	■	■	▨	▨	□	▨
	+	▨	■	■	▨	▨	□	▨

Sensitivity index
■ > 3 (high)
▨ 0-3 (low)
□ 0 (none)

Fig. 7. Graphical summary of the sensitivity analysis. Model parameters and environmental variables tested for sensitivity are presented on the vertical dimension, and the model-predicted optima of time of birth and vertical strategy, and the associated fitness on the horizontal dimension. +/−: 25% increase/decrease in the parameter value, E/D: 15-d earlier/delayed and S/L: 15-d shorter/longer scenarios regarding timing and duration of the productive season (see Appendix A3 in Supplementary material).

seeds using a binary (two-way) deterministic tournament selection (Goldberg and Deb, 1991; Miller and Goldberg, 1995). Genes of two randomly selected parents from the mating pool are recombined through blend crossover following the BLX-α method (Eshelman and Schaffer, 1993), which produces two offspring (recombinants). Genes of the recombinants are mutated at a probability of 0.02 by random replacement (uniform mutation: Eiben and Smith, 2003; Haupt and Haupt, 2004). The population of strategies resulting from these operations comprises of *N* parents, whose fitness is known and *N* offspring, whose fitness is not yet known. Parents with unique gene combinations are selected to construct a library (hereafter, the reference library), which is updated at each iteration. Each offspring is compared with those in the reference library to assess their fitness. Fitness of the offspring with similar gene combination to those in the library are assigned *in-situ*, while the rest goes through the life cycle simulation to determine fitness (LS-2 in Fig. 5d). Once the fitness of all 2*N* individuals are known, *N* survivors are selected following a round-robin (all-play-all) tournament of size 10 (Harik et al., 1997; Eiben and Smith, 2003). This process is repeated for a minimum of 100 iterations, and terminated when the mean fitness of the population shows no improvement for 25 consecutive iterations (ϕ in Fig. 5d, Eiben and Smith, 2003).

2.7. Programming, execution and analysis of the model

We used R version 3.3.1 (R Core Team, 2016) and R Studio integrated development environment (IDE) version 1.0.136 (RStudio Team, 2016) along with the high-performance computing packages Rcpp (Eddelbuettel et al., 2011) and bigmemory (Kane et al., 2013) to construct, simulate and analyze the model.

A basic run was performed in the Environment-L using default values for model parameters (Table 4). In order to test the influence of model parameters and environmental variables on model-predicted vertical strategies and fitness, we performed a sensitivity analysis following (Jørgensen and Bendoricchio, 2001). Here, we calculated a sensitivity score (S_x) as;

$$S_x = \frac{(X_{BR} - X_M)/X_{BR}}{(P_{BR} - P_M)/P_{BR}} \quad (16)$$

where *X* is the predicted model output of the basic run (X_{BR}) and the modified run (X_M) for a given change (±25%) of input parameter value between the basic run (P_{BR}) and the modified run (P_M). We tested the sensitivity of vertical strategies and fitness for 13 different input parameters (Appendix A3 in Supplementary material). For the convenience of interpretation of these results, we presented the sensitivity scores under three categories: no-sensitivity ($S_x = 0$), low sensitivity ($0 < S_x \leq 3$) and high sensitivity ($S_x > 3$). Finally, we

Table 6
Predicted variability of emergent behavioral strategies and life history traits (Fig. 2, Table 3) induced by model parameters and environmental variables analyzed for sensitivity (Fig. 7, Appendix A3 in Supplementary material). Only the input parameters with highest influence on fitness (sensitivity index >3) are tabulated.

Parameter	Variation	Time of birth (day)	Surface time[a] (h)	DVM amplitude[a] (m)	Onset of seasonal descent (day)	Onset of seasonal ascent (day)	Overwintering depth (m)	Development time[b] (d)	Food limitation index[a]	Body mass at seasonal descent (μg C)		Onset of egg production (day)	Fecundity	Breeding mode index	Longevity (d)	Absolute fitness
										W_c	W_s					
Basic run	0%	120	20.5	5	166	92	150	68.1	0.33	120.4	195.7	114	2972	0.000	414	4.10
Visual predation risk (K)	−25%	118	22.7	3	163	91	150	65.2	0.38	127.0	203.2	111	3834	0.000	430	21.2
	+25%	123	19.8	7	168	90	170	69.4	0.29	116.0	185.6	114	1446	0.000	389	0.90
Food concentration (F)	−25%	105	22.9	3	183	85	150	98.4	0.25	221.1	342.7	105	415	0.018	384	1.00
	+25%	122	19.8	6	157	99	150	59.5	0.63	120.8	196.3	123	3957	0.000	424	8.70
Temperature	−25%	103	23.0	2	181	82	150	99.1	0.21	229.7	346.3	103	654	0.022	387	1.20
	+25%	127	19.7	7	160	107	150	47.0	0.68	124.4	202.5	121	5285	0.000	412	16.1

W_c = structural mass, W_s = mass of energetic reserve.
[a] Mean of all stages.
[b] From egg to adult excluding the overwintering period.

studied the changes of heuristically optimized vertical strategies by performing model simulations in the three model environments at different levels of visual predation risk, while maintaining the rest of the parameter values at its default levels.

As GAs produce heuristic estimates of the maximum fitness, there is no guarantee that it would converge on the global maximum given a potentially diverse fitness landscape (Record et al., 2010). Therefore, we replicated each model run 10 times with different starting values assigned to the soft parameters (Table 2) to check if the algorithm converges on the same set of solutions. As the optimized parameter values showed little variability between replicate runs (<5%), we used the mean of the replicates for each parameter for analyses.

3. Results

3.1. The basic run

In the basic run, the life cycle emerging from the model began as an egg spawned at 20 m depth in late-April. The first two nauplii stages did not perform DVM, but DVM and the associated metabolic cost (swimming cost) increased ontogenetically from NIII onwards (Fig. 6a, b, e and f). The somatic growth of all developmental stages beyond NV occurred under food limitation (Fig. 6c), and because of reduced growth rates, their predicted development times were higher than those estimated from Bělehrádek temperature functions (Fig. 6d). As the energetic reserve reached 65% of the total body mass ($W_S \approx 196$ μg C, Fig. 6g), the developmental stage CV descended to an overwintering depth of 150 m in mid-June, ca. 2 months before the pelagic primary production had terminated (Fig. 6e). It remained there for ca. 290 days, and ascended into near-surface waters again in early-April of the following year, ca. 10 days after the pelagic primary production had commenced (Fig. 1c), with fully depleted energetic reserves. Although the energetic cost of seasonal migration was quite high, the cost of ascent was ca. ¼ of that of the descent due to the loss of body mass during overwintering (Fig. 6f and g). The copepod developed to an adult female in mid-April, and thenceforth produced eggs (ca. 3000) via income breeding until mid-June and then died (Fig. 6h).

3.2. Sensitivity analysis

The model-predicted fitness was highly sensitive to visual predation risk, food concentration and temperature (Fig. 7). A 25% change in the visual predation risk ($K = 7.5 \times 10^{-3}$ and 1.25×10^{-2}) influenced the DVM, which intensified at the higher-end of K and vice versa (Table 6). Although the overwintering depth deepened by ca. 13% under higher visual predation risk, it did not change under lower visual predation risk. Furthermore, higher visual predation risk lowered the fecundity and longevity, and vice versa (Table 6).

A 25% change in food concentration ($F = 10$ and 6 mg m^{-3} Chl.-a) notably influenced the DVM, timing of SVM and time of birth, but not the overwintering depth (Fig. 7). Under low food concentration, the DVM was less pronounced and the seasonal descent was delayed ca. 15 d compared to the basic run, possibly because of foraging later into the feeding season due to lower growth potential sustained under increased food limitation (Table 6). However, the copepod overwintered as a significantly large CV with elevated energetic reserves, and made ca. 7-d earlier spring ascent (late March), followed by spawning that preceded the pelagic bloom by ca. 2 days (cf. Fig. 1c). Here, ca. 2% of the total egg production was sourced from capital breeding (Table 6). Early seasonal ascent, capital breeding and early spawning thus appear as strategies employed to avoid seasonal peak in visual predation risk (cf. Fig. 1a, Eqs. (9) and (10)) when foraging efforts are elevated to cope with lower

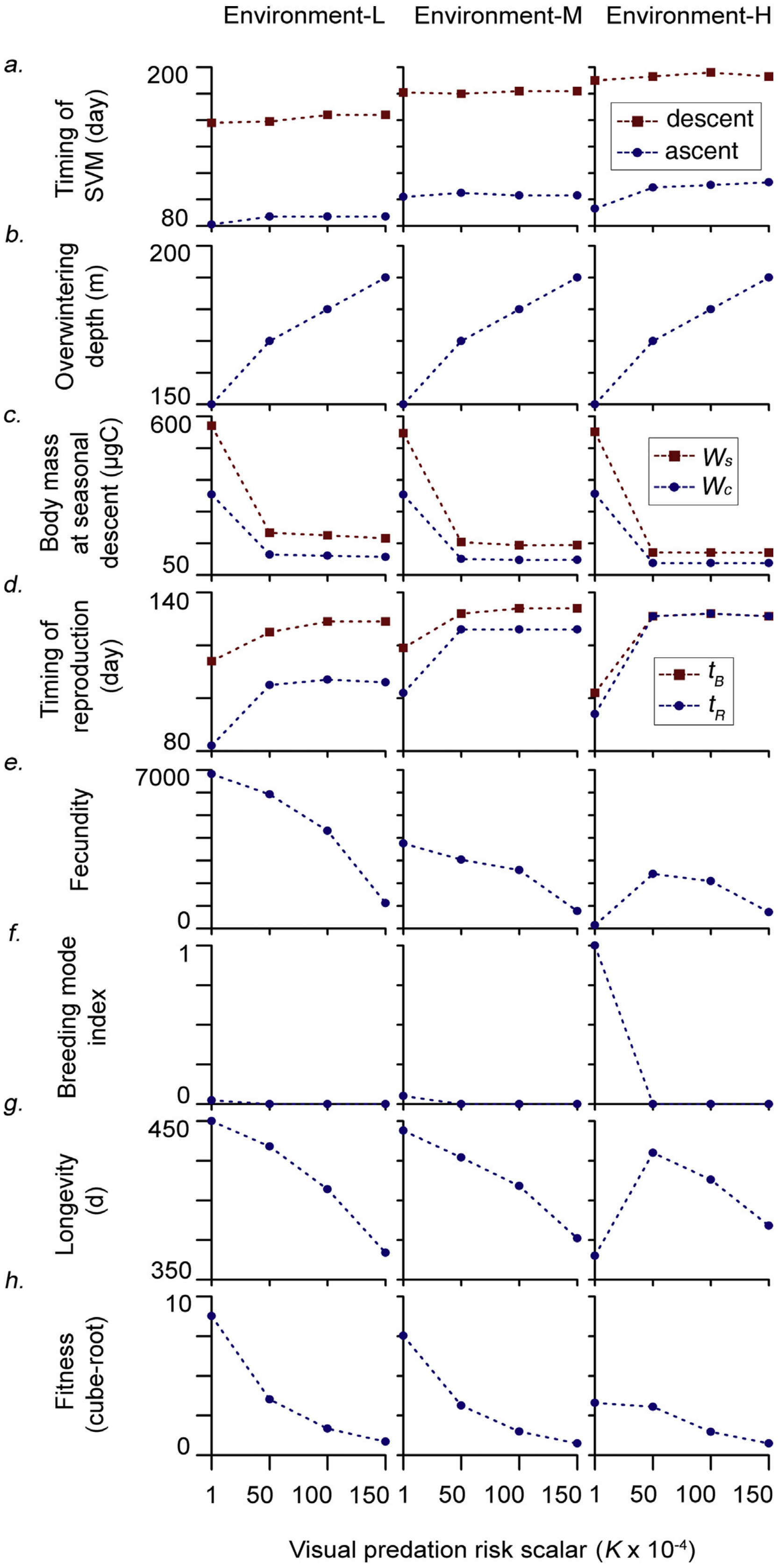

Fig. 8. Predicted optima of time of birth (t_B), vertical strategy and associated life history traits of the copepod in the three model environments under variable levels of visual predation risk. Visual predation risk is scaled by varying the parameter K in a range of $1–150 \times 10^{-4}$. The fitness is cube-root transformed for the convenience of visualization. Time is presented as day of the year, where day 1 = 1 January. W_c and W_s are structural and energy reserve masses, and t_R is time of first reproduction.

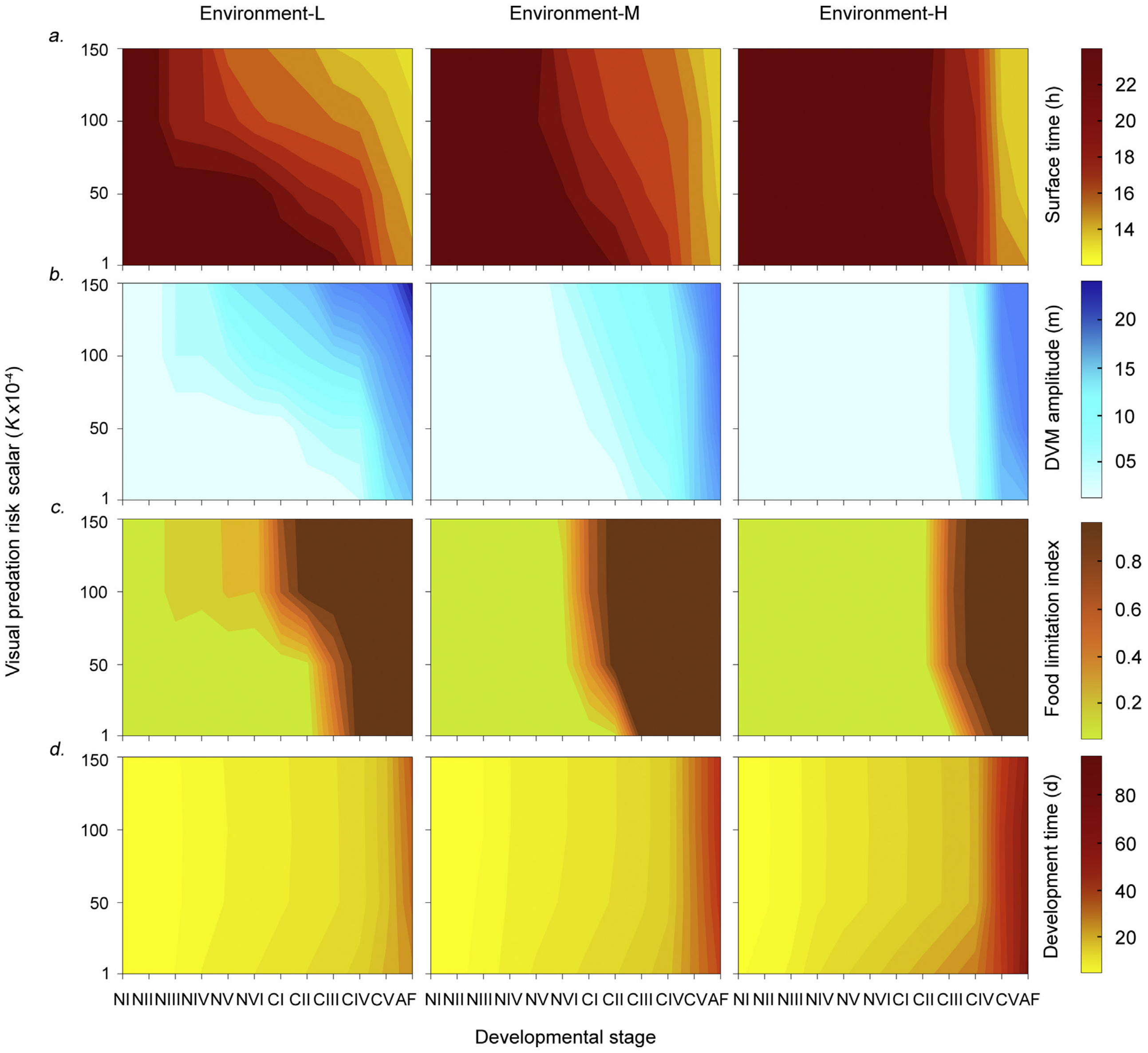

Fig. 9. Predicted stage-specific surface time (a), DVM amplitude (b), food limitation index (c) and the development times (egg to a given stage excluding the overwintering period, d) of the copepod in the three model environments under variable levels of visual predation risk.

growth potential. However, this came with a cost of decreased fecundity (80%) and longevity (7%) (Fig. 7, Table 6). Increased food concentration had the opposing effects on the predicted behavioral strategies and life history traits described above (Fig. 7, Table 6).

The influence of 4.5 °C change in temperature (T = 22.5 and 13.5 °C) on copepod's behavior and life history followed the same general trends described for food concentration (Fig. 7, Table 6), and highlight the equally important roles played by food availability and temperature in growth and development.

3.3. Latitudinal environmental variability and visual predation risk

Model-predicted optimal time of birth, body mass (W_c and W_s) at seasonal descent, overwintering depth and longevity changed with visual predation risk (K), but showed less variability along the modelled latitudinal environmental gradient (Fig. 8b–d and g). The predicted optimal time of birth changed from late-April to mid-May with increasing visual predation risk, and was constant across the three model environments, with the exception that it occurred the earliest in mid-April at Environment-H under the lowest visual predation risk ($K = 10^{-4}$, Fig. 8d). At lower levels of visual predation risk, the copepod overwintered as relatively large CVs with elevated energetic reserves at relatively shallow depths (Fig. 8b and c). However, as the visual predation risk increased, the copepod overwintered as smaller CVs or CIVs with relatively less energetic reserves at greater depths. Although the predicted longevity decreased by ca. 80 d along the modelled visual predation risk gradient (Fig. 8g), longevity at Environment-H under $K = 10^{-4}$ was lower (365 d) compared to those predicted under higher visual predation risk levels (384–430 d).

The predicted timing of SVM showed significant variability across the three model environments, but was less affected by visual predation risk (Fig. 8a). Both the descent and ascent occurred earliest at the lowest latitude environment, but happened later in the season at higher-latitude environments, with a shift of about a month. Although this reflects the delayed occurrence of the pelagic bloom along the modelled latitudinal gradient (Fig. 1c, f and i, Appendix A1 in Supplementary material), the seasonal ascent at Environment-H under lowest visual predation risk ($K = 10^{-4}$) occurred ca. 25 days before the pelagic primary production had commenced (Figs. 1i and 8a).

The predicted onset of spawning, fecundity and breeding mode index (Fig. 8d–f), along with the predicted timing and amplitude of DVM, food limitation index and development time (Fig. 9) varied with both the visual predation risk and latitudinal environmental gradient. In all model environments, the spawning started earliest under the lowest visual predation risk ($K = 10^{-4}$, Fig. 8d). Here, spawning commenced ca. 5–7 days earlier than the onset of spring primary production in lower latitude environments (Fig. 1c and f), and ca. 2.5–5% of the total egg production were sourced from capital breeding (Fig. 8f). Spawning at Environment-H commenced ca. 25 d prior to the pelagic bloom, but lasted only for ca. 10 days (Figs. 1i, 8d and g). Consequently, the expected fecundity was the lowest (ca. 145 eggs, Fig. 8e) and all eggs were sourced from capital breeding (Fig. 8f). The onset of spawning shifted later into the season at higher latitude model environments at higher levels of visual predation risk, and occurred after the commencement of the pelagic primary production (Figs. 1c, f, i and 8d). Here, all eggs were produced via income breeding (Fig. 8f). At lower levels of visual predation risk ($10^{-4} \leq K \leq 5 \times 10^{-3}$), the predicted DVM pattern was similar across the three model environments, where developmental stages until early copepodites did not perform DVM (Fig. 9a and b). Although the model predicted the younger developmental stages (NIII onwards) to perform DVM under elevated visual predation risk at Environment-L, this effect gradually waned in higher-latitude model environments. The food limitation index strongly followed the DVM pattern, where developmental stages that performed DVM suffered from increased food limitation (Fig. 9c). Food limitation significantly reduced the growth rates (cf. Eqs. (1)–(3), see also Appendix A4 in Supplementary material), and consequently, the development times increased along the modelled environmental gradient (Fig. 9d). Further, in each model environment, lowest development times were predicted under the lowest level of visual predation risk.

4. Discussion

4.1. Influence of environmental variables on vertical strategies

4.1.1. Diel vertical migration

In this model, visual predation risk had the highest influence on the DVM, which diminished under low visual predation risk (Figs. 7 and 9, Table 6) and completely ceased when visual predation was removed from the model ($K = 0$, data not presented). Conversely, under high visual predation risk, also younger developmental stages reduced the time spent in food-rich surface waters by performing low-amplitude (shallow) DVM (Fig. 9a and b). Food concentration and temperature also influenced the DVM (Fig. 7, Table 6). Lower food concentrations or temperatures produced low-amplitude DVM, possibly due the low growth potential attained in cold, food-limited conditions (Fig. 9, Eqs. (1)–(8), Appendix A4 in Supplementary material). Under these conditions, it appears that modelled copepods do not possess sufficient growth potential to trade off for survival and perform high-amplitude (deep) DVM, a conclusion also drawn in empirical work (e.g. Huntley and Brooks, 1982; Loose and Dawidowicz, 1994). Reduced or absence of DVM under low food concentrations and temperatures are reported from several other modeling studies on copepods and euphausiids (e.g. Andersen and Nival, 1991; Fiksen and Giske, 1995; Fiksen and Carlotti, 1998; Tarling et al., 2000) and from empirical work on marine copepods and freshwater cladocerans (e.g. Hardy and Gunther, 1935; Huntley and Brooks, 1982; Johnsen and Jakobsen, 1987). However, the largely exogenous-regulated DVM behavior emerging from this model does not render a complete view on the subject matter, as DVM can also be sensitive to internal (physiological) states of zooplankton (e.g. hunger and satiation, Hays et al., 2001; Pearre, 2003).

The effect of temperature on growth potential further explains the diminished influence of visual predation risk on the timing and amplitude of DVM predicted at higher latitude model environments (Fig. 9). Albeit similar food concentrations, the modelled temperatures decreased from lower- to higher-latitude model environments, reflecting a decreasing gradient of growth potential (Fig. 1, Appendix A4 in Supplementary material). Consequently, the model-predicted optimal DVM strategy for higher-latitude environments was to elevate the growth potential by spending more time foraging in near-surface waters (Fig. 9a and b). This effect was most pronounced among younger developmental stages (NIII–CI), whose DVM reduced from environment-L to -M, and completely ceased at environment-H. DVM of younger developmental stages (NIII onwards) are most commonly reported from lower latitudes for *Calanus* spp. (e.g. Huntley and Brooks, 1982; Uye et al., 1990; Huang et al., 1993; Osgood and Frost, 1994; Zakardjian et al., 1999) and *Metridia* spp. (e.g. Hays, 1995). While some field studies failed to detect notable DVM in high-latitudes (e.g. Blachowiak-Samolyk et al., 2006; Basedow et al., 2010), others reported ontogenetic increase of DVM (CI onwards, e.g. Dale and Kaartvedt, 2000; Daase et al., 2008) in *Calanus* spp. However, empirical data with high spatial, temporal and biological (i.e. developmental stage) resolution is needed to test the ontogenetic and latitudinal patterns of DVM predicted by our model.

The predicted DVM amplitudes spanned across the productive part of the water column (i.e. upper 30 m, cf. Figs. 1, 6 and 9), and showed a positive relationship with the vertical extent of food availability (Fig. 7). Moreover, strategies that involve higher-amplitude DVM lead to increased food-limitation, where younger developmental stages with no energetic reserves tend to suffer from starvation risk due to low temperatures and food concentrations that prevail in deeper parts of the model environments (Fig. 1). Therefore, low-amplitude DVM appears to be a strategy that efficiently trades off growth potential for survival, by balancing both the visual predation and starvation risks (Kerfoot, 1970; Fiksen and Giske, 1995; De Robertis, 2002). Although higher-amplitude DVM can be predicted either by not modeling starvation risk or imposing starvation tolerance (e.g. Andersen and Nival, 1991; Carlotti and Wolf, 1998; Zakardjian et al., 1999; Tarling et al., 2000), we did not follow these approaches because our model sufficiently represents the relative importance of DVM across the modelled environmental gradients.

4.1.2. Seasonal vertical migration

Food availability and temperature had the most notable influence on the model-predicted timing of SVM (Fig. 7, Table 6). The predicted shift in timing of seasonal descent and ascent coincided with those of the pelagic algal bloom and thermal stratification along the modelled latitudinal gradient (Figs. 1 and 8a). This agrees with the argument that food availability is the ultimate factor influencing the timing of seasonal vertical migration of *Calanus* spp. (Herman, 1983; Head and Harris, 1985; Hind et al., 2000). However, field estimates of timing of SVM of *Calanus* spp. from low to high latitudes do not point to a simple south–north gradient as predicted in our model (Table 7, see also Melle et al., 2014). This discrepancy of model predictions and field estimates underlies the differences between location-specific variability in hydrography, algal bloom dynamics and species composition (e.g. Hirche, 1991; Daase et al., 2013), diversity of generation lengths and breeding strategies (e.g. Conover, 1988; Falk-Petersen et al., 2009) and climate-driven and other stochastic oscillations of environmental

Table 7
Timing of seasonal ascent and descent of *Calanus* spp. estimated by several high-latitude field investigations. These estimates are based on observation of zooplankton populations oftentimes containing various combinations of *C. helgolandicus*, *C. finmarchicus*, *C. glacialis* and *C. hyperboreus*. Geographical location is approximate. Data for North-Atlantic are available in Melle et al. (2014).

Study	Lat.	Lon.	Onset of descent	Onset of ascent
Hirche (1984)	58° N	11° E	mid-October	mid-May
Bagøien et al. (2000)	59° N	10° E	July–August	March
Heath (1999)	61° N	4° W	–	May
Gislason and	62° N	20° W	–	April
Astthorsson (2000)	64° N	28° W	–	April
Østvedt (1955)	66° N	2° E	July	April
Kosobokova (1999)	66° N	35° E	mid-July	mid-May
Astthorsson and Gislason (2003)	68° N	13° E	–	May
Madsen et al. (2001)	69° N	54° W	–	mid-April
Madsen et al. (2008)	69° N	54° W	late-September	early-April
Hirche (1997)	71° N	4° E	July–August	April
	74° N	1° E	July–August	April
Unstad and Tande (1991)	75° N	30° E	–	May
Arashkevich et al. (2002)	76° N	33° E	July	May
Hirche and Kosobokova (2011)	77° N	25° E	–	March
Hirche and Kosobokova (2003)	78° N	82.5° E	–	mid-May
Bandara et al. (2016)	78° N	16° E	July–August	mid-February
Dawson (1978)	84° N	112° W	August	June

conditions (e.g. Reid et al., 1998; Eiane and Parisi, 2001; Ji, 2011). However, direct comparisons between vertical migratory patterns predicted by a strategy-oriented model and field estimates should be done with caution, as an environment-specific optimal vertical strategy predicted by the model contrasts the diversity of vertical behavior exhibited by individuals of a zooplankton population.

Visual predation risk and depth of thermal stratification (summer–autumn) were the only environmental variables that influenced the model-predicted overwintering depth (Figs. 7 and 8b, Table 6). The overwintering depth deepened at higher levels of visual predation risk and deeper thermal stratification depths, and agrees with Hirche (1991), Kaartvedt (1996), Dale et al. (1999), Bagøien et al. (2000) and Astthorsson and Gislason (2003) that *Calanus* spp. prefer colder water masses with low predator abundance for overwintering. However, the overwintering depths predicted by or model underestimate those of field observations, which can extend well below 1000 m (e.g. Østvedt, 1955). Apart from the shallow bottom depths modelled, this discrepancy largely reflects how overwintering habitat selection of *Calanus* spp. is influenced by the buoyancy-effect of stored lipid reserves (Visser and Jónasdóttir, 1999), convective mixing of surface waters (Irigoien, 2004) and vertical distribution of water masses and predator populations, such as mesopelagic fish, predatory ctenophores and krill (Hirche, 1991; Kaartvedt 1996; Bagøien et al., 2000; Bandara et al., 2016).

4.2. *Influence of vertical strategies on fitness and phenology*

4.2.1. *Diel vertical migration*

In the model, high-amplitude DVM caused increased food limitation that led to slow growth and development and reduced fecundity (Figs. 7 and 9, Table 6). This ultimately resulted in lower fitness relative to that predicted for low-amplitude DVM. It is therefore apparent that decisions to fully or partly disregard DVM in models focusing SVM and other seasonal strategies should be made with caution, as our findings indicate that DVM can have a notable negative influence on growth and development of younger developmental stages, especially at lower latitudes.

At higher levels of visual predation risk, the model predicted up to a one month delay in the onset of spawning (Fig. 8d), and highlights the influence of predation risk on the reproductive phenology (Magnhagen, 1991; Stibor, 1992; Varpe et al., 2007). These late-spawned copepods appeared to possess higher fitness compared to those spawned earlier (Fig. 8h). This seems counterintuitive as zooplankton are more vulnerable to visual predation risk later in the season due to the higher irradiance levels that persist in late-spring and summer. In this model, the early feeding season (i.e. until the time of peak pelagic bloom) is characterized by higher food concentrations and lower temperatures (Fig. 1). Although the food concentration decreases by ca. 20% by late spring or early-summer, the ambient temperature increases by ca. 2–4 times. Further, even at the onset of the productive season, the visual predation risk had reached ca. 70% of its maximum in all model environments (Fig. 1a, d and g). Therefore, it is likely that copepods born relatively later in the season use the higher temperatures to attain a higher growth (Eqs. (1)–(8), Appendix A4 in Supplementary material), which is then efficiently traded off for survival through DVM to counter the risk of increasing visual predation risk (Fig. 9). Conversely, due to lower temperatures, copepods born earlier in the season must elevate the time spent foraging in near-surface waters to attain higher growth rates, and become more vulnerable to visual predation risk. However, it should be noted that our model does not consider the ability of *Calanus* spp. to use the darker and seasonally ice-covered period of the year to attain growth with minimal influence from visual predators by feeding on alternative food sources, such as ice algae and microzooplankton (Conover and Siferd, 1993; Søreide et al., 2010).

Compared to the phenology of reproduction, the elevated visual predation risk had little influence on the timing of seasonal migration (Fig. 8a). The SVM strategy predicted by the model was to descend to overwintering depth approximately at the same period of the year (mid–late summer), but with ca. ⅓ lesser the body mass (both structural and energetic reserve mass) compared to that under the lowest visual predation risk (Fig. 8a and c). As higher visual predation risk tends to intensify DVM in this model (Fig. 9a and b), it appears that trading off growth potential for survival makes an earlier seasonal descent unfavorable, as food-limitation and slower growth rates (Fig. 9c and d) demands more time to acquire sufficient energy reserves to overwinter, despite the smaller body mass of the overwintering stage. Further, as the model-predicted body mass of the overwintering stage reaches a lower threshold at $K > 10^{-4}$ (Fig. 8c), it is likely that modelled copepods overwintered with minimum reserves to last the overwintering duration, and therefore makes an earlier descent (with lesser energy reserves) nearly impossible. In the contrary, occupying near-surface waters later into the season and descend to overwintering depths with elevated energetic reserves is also unfavorable as the visual predation risk in this model is not nullified even at the deepest parts of the water column (Eq. (10)). The lesser influence of visual predation risk on the timing of SVM does not align with Kaartvedt (2000) and Varpe and Fiksen (2010) who view predation by planktivorous fish as a key driver of generation lengths and timing of seasonal descent in *C. finmarchicus* in the Norwegian Sea. However, the consequences of DVM on the timing of seasonal descent presented here may diminish if there is an energetic benefit of DVM (e.g. McLaren, 1963; Enright, 1977), if copepods are capable of utilizing alternative food sources (e.g. Runge and Ingram, 1991; Hirche and Kwasniewski, 1997) or if there is a strong size selection against larger developmental stages by visual predators than the linear relationship applied in our model (cf. Fig. 4a with Brooks and Dodson, 1965; Batty et al., 1990; Langbehn and Varpe, 2017).

4.2.2. Seasonal vertical migration

SVM was essential for the wintertime survival of the modelled copepods, given its food source is only available during the primary production season (spring–autumn, Fig. 1). Different combinations of proxies (Table 2) yielded non-seasonally migrating strategies, in which the copepods developed to adults and reproduced within the same productive season. Although this strategy had the potential to produce more than one generation per year (especially in the relatively lower-latitude environment-L, Fig. 1a–c), we did not peruse this further, as our focus was on an annual life cycle (see the fitness weighing process, Eq. (14), Fig. 5a–c).

The body mass and the size of energetic reserve at seasonal descent together with the timing of seasonal ascent had a profound influence on the predicted timing of reproduction, breeding strategy and fecundity (Fig. 8). Overwintering as large CVs with elevated energetic reserves at lower visual predation risk enabled the copepod to allocate the post-overwintering surplus energetic reserves to capital breeding in the following year (Fig. 8c and f, and see also Sainmont et al., 2014a; Ejsmond et al., 2015; Halvorsen, 2015). As capital breeding emerged in environments with lower temperatures and food concentrations (Fig. 7, Table 6), it appears as a strategy that allows the new generation to feed from the very start of the feeding season, while avoiding the seasonal peak in visual predation risk later in the year (Fig. 1, see also Varpe et al., 2009). The proportional increase of capital breeding eggs from relatively lower-latitude environment-L to higher-latitude environment-H reflects the decreasing temperature gradient that occur at overwintering depths of these environments (Figs. 1, 8b and f). Overwintering in colder water masses reduces the metabolic costs and conserves the energetic reserve, which ultimately boosts the fecundity through capital breeding (Hirche, 1991; Hirche, 1996; Astthorsson and Gislason, 2003). The pure capital breeding strategy predicted at environment-H under the lowest visual predation risk more resembles the spawning strategy of *C. hyperboreus* than *C. finmarchicus* and *C. glacialis* (Conover, 1988; Falk-Petersen et al., 2009). The sensitivity of the model-predicted breeding strategy to visual predation risk indicates an extensive pre-breeding cost of capital breeding imposed by the size-dependent visual predation risk and acquisition and carriage of energy reserves (Jönsson, 1997; Varpe et al., 2009). Moreover, excess energy storage (i.e. more than to overwinter) and capital breeding do not emerge as dominant strategies in this model as the environmental parameters are modelled in a perfectly predictable manner, without any year-to-year variability. However, capital breeding and energy storage may possess a much larger adaptive significance in nature, where spatio-temporal environmental heterogeneity and unpredictability are more pronounced compared to our model (e.g. Jönsson, 1997; Fischer et al., 2009).

4.3. Concluding remarks

Findings of this study highlight the influence of environmental variables on vertical strategies, and suggest that in seasonal environments, DVM and SVM should be studied in concert, as these behavioral strategies can have profound and largely different effects on fitness and phenology of herbivorous zooplankton. Therefore, given the significance of biological information ensued, sacrificing computer time to adopt higher spatio-temporal resolution in behavioral and life-history models seems to be an appealing practice. However, strong recommendations should only be made after testing our model predictions further, especially, through improvements to cope with environmental stochasticity (e.g. Eiane and Parisi, 2001; Ji, 2011), and to incorporate the plasticity of feeding strategies, generation times and body sizes of *Calanus* spp. (e.g. Broekhuizen et al., 1995; Fuchs and Franks, 2010; Ji et al., 2012; Banas et al., 2016).

Acknowledgements

This project was funded by VISTA (project no. 6165), a basic research program in collaboration between The Norwegian Academy of Science and Letters and Statoil. ØV received funding from the Fulbright Arctic Initiative and thanks the Woods Hole Oceanographic Institution for hosting during the Fulbright exchange. Authors are also thankful to the two anonymous reviewers for critically reading the earlier draft of the manuscript and suggesting substantial improvements.

Appendix A. Supplementary data

Supplementary data associated with this article can be found, in the online version, at https://doi.org/10.1016/j.ecolmodel.2017.12.010.

References

Aidley, D., 1981. Questions about migration. In: Aidley, D. (Ed.), Animal Migration, vol. 2. Press Syndicae of the University of Cambridge, New York, USA, pp. 1–9.

Alerstam, T., Hedenström, A., Åkesson, S., 2003. Long-distance migration: evolution and determinants. Oikos 103, 247–260, http://dx.doi.org/10.1034/j.1600-0706.2003.12559.x.

Andersen, V., Nival, P., 1991. A model of the diel vertical migration of zooplankton based on euphausiids. J. Mar. Res. 49, 153–175, http://dx.doi.org/10.1357/002224091784968594.

Arashkevich, E., Wassmann, P., Pasternak, A., Riser, C.W., 2002. Seasonal and spatial changes in biomass, structure, and development progress of the zooplankton community in the Barents Sea. J. Mar. Syst. 38, 125–145, http://dx.doi.org/10.1016/S0924-7963(02)00173-2.

Astthorsson, O.S., Gislason, A., 2003. Seasonal variations in abundance, development and vertical distribution of *Calanus finmarchicus*, *C. hyperboreus* and *C. glacialis* in the East Icelandic Current. J. Plankton Res. 25, 843–854, http://dx.doi.org/10.1093/plankt/25.7.843.

Båmstedt, U., Eilertsen, H.C., Tande, K.S., Slagstad, D., Skjoldal, H.R., 1991. Copepod grazing and its potential impact on the phytoplankton development in the Barents Sea. Polar Res. 10, 339–354, http://dx.doi.org/10.1111/j.1751-8369.1991.tb00658.x.

Båtnes, A.S., Miljeteig, C., Berge, J., Greenacre, M., Johnsen, G.H., 2015. Quantifying the light sensitivity of *Calanus* spp. during the polar night: potential for orchestrated migrations conducted by ambient light from the sun, moon, or aurora borealis? Polar Biol. 38, 51–65, http://dx.doi.org/10.1007/s00300-013-1415-4.

Bagøien, E., Kaartvedt, S., Øverås, S., 2000. Seasonal vertical migrations of *Calanus* spp. in Oslofjorden. Sarsia 85, 299–311, http://dx.doi.org/10.1080/00364827.2000.10414581.

Banas, N.S., Møller, E.F., Nielsen, T.G., Eisner, L.B., 2016. Copepod life strategy and population viability in response to prey timing and temperature: testing a new model across latitude, time, and the size spectrum. Front. Mar. Sci. 3, 225, http://dx.doi.org/10.3389/fmars.2016.00225.

Bandara, K., Varpe, Ø., Søreide, J.E., Wallenschus, J., Berge, J., Eiane, K., 2016. Seasonal vertical strategies in a high-Arctic coastal zooplankton community. Mar. Ecol. Prog. Ser. 555, 49–64, http://dx.doi.org/10.3354/meps11831.

Banse, K., 1964. On the vertical distribution of zooplankton in the sea. Prog. Oceanogr. 2, 55–125, http://dx.doi.org/10.1016/0079-6611(64)90003-5.

Basedow, S.L., Tande, K.S., Stige, L.C., 2010. Habitat selection by a marine copepod during the productive season in the Subarctic. Mar. Ecol. Prog. Ser. 416, 165–178, http://dx.doi.org/10.3354/meps08754.

Batty, R., Blaxter, J., Richard, J., 1990. Light intensity and the feeding behaviour of herring, *Clupea harengus*. Mar. Biol. 107, 383–388, http://dx.doi.org/10.1007/BF01313419.

Berge, J., et al., 2009. Diel vertical migration of Arctic zooplankton during the polar night. Biol. Lett. 5, 69–72, http://dx.doi.org/10.1098/rsbl.2008.0484.

Berge, J., Varpe, Ø., Moline, M.A., Wold, A., Renaud, P.E., Daase, M., Falk-Petersen, S., 2012. Retention of ice-associated amphipods: possible consequences for an ice-free Arctic Ocean. Biol. Lett. 8, 1012–1015, http://dx.doi.org/10.1098/rsbl.2012.0517.

Bianchi, D., Mislan, K., 2016. Global patterns of diel vertical migration times and velocities from acoustic data. Limnol. Oceanogr. 61, 353–364, http://dx.doi.org/10.1002/lno.10219.

Bianchi, D., Galbraith, E.D., Carozza, D.A., Mislan, K., Stock, C.A., 2013. Intensification of open-ocean oxygen depletion by vertically migrating animals. Nat. Geosci. 6, 545–548, http://dx.doi.org/10.1038/ngeo1837.

Blachowiak-Samolyk, K., et al., 2006. Arctic zooplankton do not perform diel vertical migration (DVM) during periods of midnight sun. Mar. Ecol. Prog. Ser. 308, 101–116, http://dx.doi.org/10.3354/meps308101.

Bollens, S.M., Frost, B.W., Thoreson, D.S., Watts, S.J., 1992. Diel vertical migration in zooplankton: field evidence in support of the predator avoidance hypothesis. Hydrobiologia 234, 33–39, http://dx.doi.org/10.1007/bf00010777.

Bozman, A., Titelman, J., Kaartvedt, S., Eiane, K., Aksnes, D.L., 2017. Jellyfish distribute vertically according to irradiance. J. Plankton Res. 39, 280–289, http://dx.doi.org/10.1093/plankt/fbw097.

Broekhuizen, N., Heath, M.R., Hay, S.J., Gurney, W.S.C., 1995. Modelling the dynamics of the North Sea's Mesozooplankton. Neth. J. Sea Res. 33, 381–406, http://dx.doi.org/10.1016/0077-7579(95)90054-3.

Brooks, J.L., Dodson, S.I., 1965. Predation, body size, and composition of plankton. Science 150, 28–35, http://dx.doi.org/10.1126/science.150.3692.28.

Burrows, M.T., Tarling, G., 2004. Effects of density dependence on diel vertical migration of populations of northern krill: a genetic algorithm model. Mar. Ecol. Prog. Ser. 277, 209–220, http://dx.doi.org/10.3354/meps277209.

Campbell, R.G., Wagner, M.M., Teegarden, G.J., Boudreau, C.A., Durbin, E.G., 2001. Growth and development rates of the copepod *Calanus finmarchicus* reared in the laboratory. Mar. Ecol. Prog. Ser. 221, 161–183, http://dx.doi.org/10.3354/meps221161.

Carlisle, D.B., Pitman, W.J., 1961. Diapause, neurosecretion and hormones in copepoda. Nature 190, 827–828, http://dx.doi.org/10.1038/190827b0.

Carlotti, F., Wolf, K.U., 1998. A Lagrangian ensemble model of *Calanus finmarchicus* coupled with a 1D ecosystem model. Fish Oceanogr. 7, 191–204, http://dx.doi.org/10.1046/j.1365-2419.1998.00085.x.

Chossat, C., 1843. Recherches expérimentales sur l'inanition. Imprimerie Royale, Paris, France.

Clarke, G.L., 1933. Diurnal migration of plankton in the Gulf of Maine and its correlation with changes in submarine irradiation. Biol. Bull. 65, 402–436, http://dx.doi.org/10.2307/1537215.

Codling, E.A., 2003. Biased Random Walks in Biology. Master Thesis. The University of Leeds.

Cohen, J., Forward, R., 2009. Zooplankton Diel Vertical Migration? A review of proximate control. In: Oceanography and Marine Biology. Oceanography and Marine Biology—An Annual Review. CRC Press, pp. 77–109, http://dx.doi.org/10.1201/9781420094220.ch2.

Cohen, J., et al., 2015. Is ambient light during the high Arctic polar night sufficient to act as a visual cue for zooplankton? PLoS One 10, e0126247, http://dx.doi.org/10.1371/journal.pone.0126247.

Conover, R., Siferd, T.D., 1993. Dark-season survival strategies of coastal zone zooplankton in the Canadian Arctic. Arctic, 303–311, http://dx.doi.org/10.14430/arctic1357.

Conover, R., 1988. Comparative life histories in the genera *Calanus* and *Neocalanus* in high latitudes of the northern hemisphere. In: Biology of Copepods. Springer, pp. 127–142, http://dx.doi.org/10.1007/BF00026299.

Costello, J., 1998. Physiological response of the hydromedusa *Cladonema californicum* Hyman (Anthomedusa: Cladonemidae) to starvation and renewed feeding. J. Exp. Biol. Ecol. 225, 13–28, http://dx.doi.org/10.1016/S0022-0981(97)00204-9.

Cresswell, K.A., Satterthwaite, W.H., Sword, G.A., 2011. Understanding the evolution of migration through empirical examples. In: Milner-Gulland, E.J., Fryxell, J.M., Sinclair, A.R.E. (Eds.), Animal Migration a Synthesis, vol. 1. Oxford University Press, Oxford, U.K, pp. 7–17.

Cushing, D.H., 1951. The vertical migration of planktonic crustacea. Biol. Rev. 26, 158–192, http://dx.doi.org/10.1111/j.1469-185X.1951. tb00645.x.

Daase, M., Eiane, K., Aksnes, D.L., Vogedes, D., 2008. Vertical distribution of *Calanus* spp. and *Metridia longa* at four Arctic locations. Mar. Biol. Res. 4, 193–207, http://dx.doi.org/10.1080/17451000801907948.

Daase, M., et al., 2013. Timing of reproductive events in the marine copepod *Calanus glacialis*: a pan-Arctic perspective. Can. J. Fish. Aquat. Sci. 70, 871–884, http://dx.doi.org/10.1139/cjfas-2012-0401.

Dale, T., Kaartvedt, S., 2000. Diel patterns in stage-specific vertical migration of *Calanus finmarchicus* in habitats with midnight sun. ICES J. Mar. Sci. 57, 1800–1818, http://dx.doi.org/10.1006/jmsc.2000.0961.

Dale, T., Bagøien, E., Melle, W., Kaartvedt, S., 1999. Can predator avoidance explain varying overwintering depth of *Calanus* in different oceanic water masses? Mar. Ecol. Prog. Ser. 179, 113–121, http://dx.doi.org/10.3354/meps179113.

Darnis, G., et al., 2017. From polar night to midnight sun: Diel vertical migration, metabolism and biogeochemical role of zooplankton in a high Arctic fjord (Kongsfjorden, Svalbard). Limnol. Oceanogr. 57, 1800–1818, http://dx.doi.org/10.1006/jmsc.2000.0961.

Davis, L., 1989. Adapting operator probabilities in genetic algorithms. Proceedings of the Third International Conference on Genetic Algorithms, 61–69.

Dawidowicz, P., Loose, C.J., 1992. Cost of swimming by *Daphnia* during diel vertical migration. Limnol. Oceanogr. 37, 665–669, http://dx.doi.org/10.4319/lo.1992.37.3.0665.

Dawson, J.K., 1978. Vertical distribution of Calanus hyperboreus in the central Arctic Ocean. Limnol. Oceanogr. 23, 950–957, http://dx.doi.org/10.4319/lo.1978.23.5.0950.

De Robertis, A., 2002. Size-dependent visual predation risk and the timing of vertical migration: an optimization model. Limnol. Oceanogr. 47, 925–933, http://dx.doi.org/10.4319/lo.2000.45.8.1838.

Deb, K., 2001. Multi-objective Optimization Using Evolutionary Algorithms, vol. 16. John Wiley & Sons, New York, USA.

Devol, A.H., 1981. Vertical distribution of zooplankton respiration in relation to the intense oxygen minimum zones in two British Columbia fjords. J. Plankton Res. 3, 593–602, http://dx.doi.org/10.1093/plankt/3.4.593.

Dupont, N., Aksnes, D.L., 2012. Effects of bottom depth and water clarity on the vertical distribution of *Calanus* spp. J. Plankton Res. 34, 263–266, http://dx.doi.org/10.1093/plankt/fbr096.

Eddelbuettel, D., François, R., Allaire, J., Chambers, J., Bates, D., Ushey, K., 2011. Rcpp: seamless R and C++ integration. J. Stat. Softw. 40, 1–18, http://dx.doi.org/10.18637/jss.v040.i08.

Eiane, K., Ohman, M.D., 2004. Stage-specific mortality of *Calanus finmarchicus*, *Pseudocalanus elongatus* and *Oithona similis* on Fladen Ground, North Sea, during a spring bloom. Mar. Ecol. Prog. Ser. 268, 183–193, http://dx.doi.org/10.3354/meps268183.

Eiane, K., Parisi, D., 2001. Towards a robust concept for modelling zooplankton migration. Sarsia 86, 465–475, http://dx.doi.org/10.1080/00364827.2001.10420486.

Eiben, A.E., Smith, J.E., 2003. Introduction to Evolutionary Computing, vol. 53. Springer, Berlin, Germany.

Ejsmond, M.J., Varpe, Ø., Czarnoleski, M., Kozłowski, J., 2015. Seasonality in offspring value and trade-offs with growth explain capital breeding. Am. Nat. 186, E111–E125, http://dx.doi.org/10.1086/683119.

Ekvall, M.T., Hylander, S., Walles, T., Yang, X., Hansson, L.A., 2015. Diel vertical migration, size distribution and photoprotection in zooplankton as response to UV-A radiation. Limnol. Oceanogr. 60, 2048–2058, http://dx.doi.org/10.1002/lno.10151.

Enright, J., 1977. Diurnal vertical migration: adaptive significance and timing. Part 1. Selective advantage: a metabolic model. Limnol. Oceanogr. 22, 856–872, http://dx.doi.org/10.4319/lo.1977.22.5.0856.

Eshelman, L.J., Schaffer, J.D., 1993. Real-coded genetic algorithms and interval-schemata. Found. Genet. Algorithm 2, 187–202, http://dx.doi.org/10.1016/B978-0-08-094832-4.50018-0.

Falk-Petersen, S., Mayzaud, P., Kattner, G., Sargent, J.R., 2009. Lipids and life strategy of Arctic *Calanus*. Mar. Biol. Res. 5, 18–39, http://dx.doi.org/10.1080/17451000802512267.

Fiksen, Ø., Carlotti, F., 1998. A model of optimal life history and diel vertical migration in *Calanus finmarchicus*. Sarsia 83, 129–147, http://dx.doi.org/10.1080/00364827.1998.10413678.

Fiksen, Ø., Giske, J., 1995. Vertical distribution and population dynamics of copepods by dynamic optimization. ICES J. Mar. Sci. 52, 483–503, http://dx.doi.org/10.1016/1054-3139(95)80062-X.

Fischer, B., Taborsky, B., Dieckmann, U., 2009. Unexpected patterns of plastic energy allocation in stochastic environments. Am. Nat. 173, E108–E120, http://dx.doi.org/10.1086/596536.

Foulds, J., Roff, J.C., 1976. Oxygen consumption during simulated vertical migration in *Mysis relicta* (Crustacea, Mysidacea). Can. J. Zool. 54, 377–385, http://dx.doi.org/10.1139/z76-042.

Frank, T.M., Widder, E.A., 1997. The correlation of downwelling irradiance and staggered vertical igration patterns of zooplankton in Wilkinson Basin, Gulf of Maine. J. Plankton Res. 19, 1975–1991, http://dx.doi.org/10.1093/plankt/19.12.1975.

Fuchs, H.L., Franks, P.J., 2010. Plankton community properties determined by nutrients and size-selective feeding. Mar. Ecol. Prog. Ser. 413, 1–15, http://dx.doi.org/10.3354/meps08716.

George, D., 1983. Interrelations between the vertical distribution of *Daphnia* and chlorophyll a in two large limnetic enclosures. J. Plankton Res. 5, 457–475, http://dx.doi.org/10.1093/plankt/5.4.457.

Gislason, A., Astthorsson, O.S., 2000. Winter distribution, ontogenetic migration, and rates of egg production of *Calanus finmarchicus* southwest of Iceland. ICES J. Mar. Sci. 57, 1727–1739, http://dx.doi.org/10.1006/jmsc.2000.0951.

Gliwicz, Z.M., 1986. A lunar cycle in zooplankton. Ecology 67, 883–897, http://dx.doi.org/10.2307/1939811.

Goldberg, D.E., Deb, K., 1991. A comparative analysis of selection schemes used in genetic algorithms. In: Rawlins, G. (Ed.), Foundations of Genetic Algorithms, vol. 1. Morgan Kaufmann Publishers, San Mateo, California, USA, pp. 69–93.

Greene, C.H., Landry, M.R., 1985. Patterns of prey selection in the cruising calanoid predator *Euchaeta elongata*. Ecology 66, 1408–1416, http://dx.doi.org/10.2307/1938003.

Grimm, V., et al., 2006. A standard protocol for describing individual-based and agent-based models. Ecol. Model. 198, 115–126, http://dx.doi.org/10.1016/j.ecolmodel.2006.04.023.

Grimm, V., Berger, U., DeAngelis, D.L., Polhill, J.G., Giske, J., Railsback, S.F., 2010. The ODD protocol: a review and first update. Ecol. Model. 221, 2760–2768, http://dx.doi.org/10.1016/j.ecolmodel.2010.08.019.

Hagen, W., Auel, H., 2001. Seasonal adaptations and the role of lipids in oceanic zooplankton. Zoology 104, 313–326, http://dx.doi.org/10.1078/0944-2006-00037.

Halvorsen, E., 2015. Significance of lipid storage levels for reproductive output in the Arctic copepod *Calanus hyperboreus*. Mar. Ecol. Prog. Ser. 540, 259–265, http://dx.doi.org/10.3354/meps11528.

Hansen, A.N., Visser, A.W., 2016. Carbon export by vertically migrating zooplankton: an optimal behavior model. Limnol. Oceanogr. 61, 701–710, http://dx.doi.org/10.1002/lno.10249.

Hardy, A., Bainbridge, R., 1954. Experimental observations on the vertical migrations of plankton animals. J. Mar. Biolog. Assoc. U. K. 33, 409–448, http://dx.doi.org/10.1017/S0025315400008456.

Hardy, A.C., Gunther, E.R., 1935. The Plankton of the South Georgia Whaling Grounds and Adjacent Waters, 1926–1927. The University Press, Cambridge, UK.

Hardy, A., 1935. The plankton community, the whale fisheries and the hypothesis of animal exclusion. Discov. Rep. 11, 273–360.

Harik, G.R., Lobo, F.G., Goldberg, D.E., 1997. The compact genetic algorithm. Urbana 51, 61801, http://dx.doi.org/10.1109/4235.797971.

Haupt, R.L., Haupt, S.E., 2004. Practical Genetic Algorithms. John Wiley & Sons, New Jersey, USA.

Hays, G., Proctor, C., John, A., Warner, A., 1994. Interspecific differences in the diel vertical migration of marine copepods: the implications of size, color, and morphology. Limnol. Oceanogr. 39, 1621–1629, http://dx.doi.org/10.4319/lo.1994.39.7.1621.

Hays, G.C., Kennedy, H., Frost, B.W., 2001. Individual variability in diel vertical migration of a marine copepod: why some individuals remain at depth when others migrate. Limnol. Oceanogr. 46, 2050–2054, http://dx.doi.org/10.4319/lo.2001.46.8.2050.

Hays, G., 1995. Ontogenetic and seasonal variation in the diel vertical migration of the copepods *Metridia lucens* and *Metridia longa*. Limnol. Oceanogr. 40, 1461–1465, http://dx.doi.org/10.4319/lo.1995.40.8.1461.

Head, E.J.H., Harris, L.R., 1985. Physiological and biochemical changes in *Calanus hyperboreus* from Jones Sound NWT during the transition from summer feeding to overwintering condition. Polar Biol. 4, 99–106, http://dx.doi.org/10.1007/BF00442907.

Heath, M.R., Jónasdóttir, S.H., 1999. Distribution and abundance of overwintering *Calanus finmarchicus* in the Faroe–Shetland Channel. Fish. Oceanogr. 8, 40–60, http://dx.doi.org/10.1046/j.1365-2419.1999.00012.x.

Heath, M.R., 1999. The ascent migration of *Calanus finmarchicus* from overwintering depths in the Faroe–Shetland Channel. Fish. Oceanogr. 8, 84–99, http://dx.doi.org/10.1046/j.1365-2419.1999.00013.x.

Herman, A.W., 1983. Vertical distribution patterns of copepods, chlorophyll, and production in northeastern Baffin Bay. Limnol. Oceanogr. 28, 709–719, http://dx.doi.org/10.4319/lo.1983.28.4.0709.

Herrera, F., Lozano, M., Verdegay, J.L., 1998. Tackling real-coded genetic algorithms: operators and tools for behavioural analysis. Artif. Intell. Rev. 12, 265–319, http://dx.doi.org/10.1023/A:1006504901164.

Heywood, K.J., 1996. Diel vertical migration of zooplankton in the Northeast Atlantic. J. Plankton Res. 18, 163–184, http://dx.doi.org/10.1093/plankt/18.2.163.

Hind, A., Gurney, W.S.C., Heath, M.R., Bryant, A., 2000. Overwintering strategies in *Calanus finmarchicus*. Mar. Ecol. Prog. Ser., 95–107, http://dx.doi.org/10.3354/meps193095.

Hirche, H.-J., Kosobokova, K., 2003. Early reproduction and development of dominant calanoid copepods in the sea ice zone of the Barents Sea—need for a change of paradigms? Mar. Biol. 143, 769–781, http://dx.doi.org/10.1007/s00227-003-1122-8.

Hirche, H.-J., Kosobokova, K., 2011. Winter studies on zooplankton in Arctic seas: the Storfjord (Svalbard) and adjacent ice-covered Barents Sea. Mar. Biol. 158, 2359–2376, http://dx.doi.org/10.1007/s00227-011-1740-5.

Hirche, H.-J., Kwasniewski, S., 1997. Distribution, reproduction and development of *Calanus* species in the Northeast water in relation to environmental conditions. J. Mar. Syst. 10, 299–317, http://dx.doi.org/10.1016/S0924-7963(96)00057-7.

Hirche, H.-J., 1984. Seasonal distribution of *Calanus finmarchicus* (Gunnerus) and *C. helgolandicus* (Claus) in a Swedish fjord. Crustaceana, 233–241.

Hirche, H.-J., 1991. Distribution of dominant calanoid copepod species in the Greenland Sea during late fall. Polar Biol. 11, 351–362, http://dx.doi.org/10.1007/BF00239687.

Hirche, H.-J., 1996. Diapause in the marine copepod, *Calanus finmarchicus*—a review. Ophelia 44, 129–143, http://dx.doi.org/10.1080/00785326.1995.10429843.

Hirche, H.-J., 1997. Life cycle of the copepod *Calanus hyperboreus* in the Greenland Sea. Mar. Biol. 128, 607–618, http://dx.doi.org/10.1007/s002270050.

Holland, J.H., 1975. Adaptation in Natural and Artificial Systems. An Introductory Analysis with Application to Biology, Control, and Artificial Intelligence. University of Michigan Press, Ann Arbor, MI.

Huang, C., Uye, S., Onbé, T., 1993. Ontogenetic diel vertical migration of the planktonic copepod *Calanus sinicus* in the Inland Sea of Japan. Mar. Biol. 117, 289–299, http://dx.doi.org/10.1007/BF00345674.

Huntley, M., Boyd, C., 1984. Food-limited growth of marine zooplankton. Am. Nat. 124, 455–478, http://dx.doi.org/10.1086/284288.

Huntley, M., Brooks, E., 1982. Effects of age and food availability on diel vertical migration of *Calanus pacificus*. Mar. Biol. 71, 23–31, http://dx.doi.org/10.1007/BF00396989.

Ingvaldsen, R., Loeng, H., 2009. Physical oceanography. In: Sakshaug, E., Johnsen, G.H., Kovacs, K. (Eds.), Ecosystem Barents Sea. Tapir Academic Press, Trondheim, Norway, pp. 33–64.

Irigoien, X., 2004. Some ideas about the role of lipids in the life cycle of *Calanus finmarchicus*. J. Plankton Res. 26, 259–263, http://dx.doi.org/10.1093/plankt/fbh030.

Iwasa, Y., 1982. Vertical migration of zooplankton: a game between predator and prey. Am. Nat. 120, 171–180, http://dx.doi.org/10.1086/283980.

Jönsson, K.I., 1997. Capital and income breeding as alternative tactics of resource use in reproduction. Oikos, 57–66, http://dx.doi.org/10.2307/3545800.

Jørgensen, S.E., Bendoricchio, G., 2001. Fundamentals of Ecological Modelling, vol. 21. Elsevier Science Ltd., Oxford, UK.

Ji, R., et al., 2012. Life history and biogeography of *Calanus* copepods in the Arctic Ocean: an individual-based modeling study. Prog. Oceanogr. 96, 40–56, http://dx.doi.org/10.1016/j.pocean.2011.10.001.

Ji, R., 2011. *Calanus finmarchicus* diapause initiation: new view from traditional life history-based model. Mar. Ecol. Prog. Ser. 440, 105–114, http://dx.doi.org/10.3354/meps09342.

Johnsen, G.H., Jakobsen, P.J., 1987. The effect of food limitation on vertical migration in *Daphnia longispina*. Limnol. Oceanogr. 32, 873–880, http://dx.doi.org/10.4319/lo.1987.32.4.0873.

Kaartvedt, S., 1996. Habitat preference during overwintering and timing of seasonal vertical migration of *Calanus finmarchicus*. Ophelia 44, 145–156, http://dx.doi.org/10.1080/00785326.1995.10429844.

Kaartvedt, S., 2000. Life history of *Calanus finmarchicus* in the Norwegian Sea in relation to planktivorous fish. ICES J. Mar. Sci. 57, 1819–1824, http://dx.doi.org/10.1006/jmsc.2000.0964.

Kane, M.J., Emerson, J.W., Weston, S., 2013. Scalable strategies for computing with massive data. J. Stat. Softw. 55, 1–19, http://dx.doi.org/10.18637/jss.v055.i14.

Kerfoot, W.B., 1970. Bioenergetics of vertical migration. Am. Nat. 104, 529–546, http://dx.doi.org/10.1086/282688.

Kiørboe, T., Hirst, A.G., 2008. Optimal development time in pelagic copepods. Mar. Ecol. Prog. Ser. 367, 15–22, http://dx.doi.org/10.3354/meps07572.

Kimmerer, W., McKinnon, A., 1987. Zooplankton in a marine bay. II. Vertical migration to maintain horizontal distributions. Mar. Ecol. Prog. Ser., 53–60.

Kosobokova, K., 1999. The reproductive cycle and life history of the Arctic copepod *Calanus glacialis* in the White Sea. Polar Biol. 22, 254–263, http://dx.doi.org/10.1007/s003000050418.

Lampert, W., 1989. The adaptive significance of diel vertical migration of zooplankton. Funct. Ecol. 3, 21–27, http://dx.doi.org/10.2307/2389671.

Langbehn, T.J., Varpe, Ø., 2017. Sea-ice loss boosts visual search: fish foraging and changing pelagic interactions in polar oceans. Glob. Change Biol. 12, 5318–5330, http://dx.doi.org/10.1111/gcb.13797.

Litchman, E., Ohman, M.D., Kiørboe, T., 2013. Trait-based approaches to zooplankton communities. J. Plankton Res. 35, 473–484, http://dx.doi.org/10.1093/plankt/fbt019.

Liu, S.-H., Sun, S., Han, B.-P., 2003. Diel vertical migration of zooplankton following optimal food intake under predation. J. Plankton Res. 25, 1069–1077, http://dx.doi.org/10.1093/plankt/25.9.1069.

Loos, M., Ragas, A.M., Plasmeijer, R., Schipper, A.M., Hendriks, A.J., 2010. Eco-SpaCE: an object-oriented, spatially explicit model to assess the risk of multiple environmental stressors on terrestrial vertebrate populations. Sci. Total Environ. 408, 3908–3917, http://dx.doi.org/10.1016/j.scitotenv.2009.11.045.

Loose, C.J., Dawidowicz, P., 1994. Trade-offs in Diel vertical migration by zooplankton: the costs of predator avoidance. Ecology 75, 2255–2263, http://dx.doi.org/10.2307/1940881.

Lucasius, C.B., Kateman, G., 1989. Application of genetic algorithms in chemometrics. In: Proceedings of the Third International Conference on Genetic Algorithms. Morgan Kaufmann Publishers Inc., pp. 170–176.

Madsen, S., Nielsen, T.G., Hansen, B.W., 2001. Annual population development and production by *Calanus finmarchicus*, *C. glacialis* and *C. hyperboreus* in Disko Bay, western Greenlan. Mar. Biol. 139, 75–93, http://dx.doi.org/10.1007/s002270100552.

Madsen, S., Nielsen, T.G., Tervo, O.M., Söderkvist, J., 2008. Importance of feeding for egg production in *Calanus finmarchicus* and *C. glacialis* during the Arctic spring. Mar. Ecol. Prog. Ser. 353, 177–190, http://dx.doi.org/10.3354/meps07129.

Magnhagen, C., 1991. Predation risk as a cost of reproduction. Trends Ecol. Evolut. 6, 183–186, http://dx.doi.org/10.1016/0169-5347(91)90210-O.

Marshall, S.M., Orr, A.P., 1972. The Biology of a Marine Copepod: *Calanus finmarchicus* (Gunnerus). Springer Science & Business Media, Berlin, Germany.

Mauchline, J., 1998. The Biology of Calanoid Copepods, vol. 33. Academic Press, San Diego, California, USA.

McLaren, I.A., 1963. Effects of temperature on growth of zooplankton, and the adaptive value of vertical migration. J. Fish. Res. Board Can. 20, 685–727, http://dx.doi.org/10.1139/f63-046.

Melle, W., et al., 2014. The North Atlantic Ocean as habitat for *Calanus finmarchicus*: environmental factors and life history traits. Prog. Oceanogr. 129, 244–284, http://dx.doi.org/10.1016/j.pocean.2014.04.026.

Miller, B.L., Goldberg, D.E., 1995. Genetic algorithms, tournament selection, and the effects of noise. Complex Syst. 9, 193–212.

Miller, C.B., Cowles, T.J., Wiebe, P.H., Copley, N.J., Grigg, H., 1991. Phenology in *Calanus finmarchicus*; hypotheses about control mechanisms. Mar. Ecol. Prog. Ser. 72, 79–91.

Miller, C.B., Lynch, D.R., Carlotti, F., Gentleman, W., Lewis, C.V., 1998. Coupling of an individual-based population dynamic model of *Calanus finmarchicus* to a circulation model for the Georges Bank region. Fish. Oceanogr. 7, 219–234, http://dx.doi.org/10.1046/j.1365-2419.1998.00072.x.

Morris, M., Gust, G., Torres, J., 1985. Propulsion efficiency and cost of transport for copepods: a hydromechanical model of crustacean swimming. Mar. Biol. 86, 283–295, http://dx.doi.org/10.1007/BF00397515.

Nival, P., Carlotti, F., Sciandra, A., 1988. Modelling of recruitment of marine species. In: Rothschild, B.J. (Ed.), Toward a Theory on Biological-Physical Interactions in the World Ocean, vol. 239. Kluwer Academic Publishers, Dordrecht, The Netherlands, pp. 321–342.

Ohman, M.D., 1990. The demographic benefits of diel vertical migration by zooplankton. Ecol. Monogr. 60, 257–281, http://dx.doi.org/10.2307/1943058.

Osgood, K.E., Frost, B.W., 1994. Ontogenetic diel vertical migration behaviors of the marine planktonic copepods *Calanus pacificus* and *Metridia lucens*. Mar. Ecol. Prog. Ser., 13–25.

Østvedt, O.J., 1955. Zooplankton investigations from weather ship M in the Norwegian Sea, 1948–49. Hvalrad Skf 40, 1–93.

Pasternak, A., Kosobokova, K., Drits, A., 1994. Feeding, metabolism and body composition of the dominant Antarctic copepods with comments on their life cycles. Russ. J. Aquat. Ecol. 3, 49–62.

Pearre, S., 1979. Problems of detection and interpretation of vertical migration. J. Plankton Res. 1, 29–44, http://dx.doi.org/10.1093/plankt/1.1.29.

Pearre, S., 2003. Eat and run? The hunger/satiation hypothesis in vertical migration: history, evidence and consequences. Biol. Rev. 78, 1–79.

R Core Team, 2016. R: A Language and Environment for Statistical Computing. 3.3.1.

RStudio Team, 2016. RStudio: Integrated Development Environment for R. 1.0.136.

Record, N., Pershing, A., Runge, J., Mayo, C.A., Monger, B.C., Chen, C., 2010. Improving ecological forecasts of copepod community dynamics using genetic algorithms. J. Mar. Syst. 82, 96–110, http://dx.doi.org/10.1016/j.jmarsys.2010.04.001.

Reid, P.C., Planque, B., Edwards, M., 1998. Is observed variability in the long-term results of the Continuous Plankton Recorder survey a response to climate change? Fish. Oceanogr. 7, 282–288, http://dx.doi.org/10.1046/j.1365-2419.1998.00073.x.

Rhode, S.C., Pawlowski, M., Tollrian, R., 2001. The impact of ultraviolet radiation on the vertical distribution of zooplankton of the genus. Daphnia Nat. 412, 69–72, http://dx.doi.org/10.1038/35083567.

Robinson, C.L.K., 1994. Modelling the Trophodynamics of a Coastal Upwelling System. Doctoral Thesis. The University of British Columbia.

Robledo, L., Soler, A., 2000. Luminous efficacy of global solar radiation for clear skies. Energy Convers. Manage. 41, 1769–1779, http://dx.doi.org/10.1016/S0196-8904(00)00019-4.

Roman, M., Smith, S., Wishner, K., Zhang, X., Gowing, M., 2000. Mesozooplankton production and grazing in the Arabian Sea. Deep Sea Res. Part II: Trop. Stud. Oceanogr. 47, 1423–1450, http://dx.doi.org/10.1016/S0967-0645(99)00149-6.

Runge, J., Ingram, R.G., 1991. Under-ice feeding and diel migration by the planktonic copepods *Calanus glacialis* and *Pseudocalanus minutus* in relation to the ice algal production cycle in southeastern Hudson Bay. Can. Mar. Biol. 108, 217–225, http://dx.doi.org/10.1007/BF01344336.

Russell, F.S., 1927. The vertical distribution of plankton in the sea. Biol. Rev. 2, 213–262, http://dx.doi.org/10.1111/j.1469-185X.1927.tb00878.x.

Sømme, J.D., 1934. Animal plankton of the Norwegian Coast Warers and the Open Sea. I—production of *Calanus finmarchicus* (Gunner) and *Calanus hyperboreus* (Krøyer) in the Lofoten Area. Fiskeridir Skr (Havunders) 4, 1–163.

Søreide, J.E., Leu, E., Berge, J., Graeve, M., Falk-Petersen, S., 2010. Timing of blooms, algal food quality and *Calanus glacialis* reproduction and growth in a changing Arctic. Glob Change Biol. 16, 3154–3163, http://dx.doi.org/10.1111/j.1365-2486.2010.02175.x.

Sainmont, J., Andersen, K.H., Varpe, Ø., Visser, A.W., 2014a. Capital versus income breeding in a seasonal environment. Am. Nat. 184, 466–476, http://dx.doi.org/10.1086/677926.

Sainmont, J., Gislason, A., Heuschele, J., Webster, C.N., Sylvander, P., Wang, M., Varpe, Ø., 2014b. Inter-and intra-specific diurnal habitat selection of zooplankton during the spring bloom observed by Video Plankton Recorder. Mar. Biol. 161, 1931–1941, http://dx.doi.org/10.1007/s00227-014-2475-x.

Sainmont, J., Andersen, K.H., Thygesen, U.H., Fiksen, Ø., Visser, A.W., 2015. An effective algorithm for approximating adaptive behavior in seasonal environments. Ecol. Model. 311, 20–30, http://dx.doi.org/10.1016/j.ecolmodel.2015.04.016.

Sakshaug, E., Johnsen, G.H., Kristiansen, S., von Quillfeldt, C., Rey, F., Slagstad, D., Thingstad, F., 2009. Phytoplankton and primary production. In: Sakshaug, E., Johnsen, G., Kovacs, K. (Eds.), Ecosystem Barents Sea. Tapir Academic Press, Trondheim, Norway, pp. 167–209.

Salzen, E., 1956. The density of the eggs of *Calanus finmarchicus*. J. Mar. Biol. Assoc. U. K. 35, 549–554, http://dx.doi.org/10.1017/S0025315400010407.

Sekino, T., Yamamura, N., 1999. Diel vertical migration of zooplankton: optimum migrating schedule based on energy accumulation. Evol. Ecol. 13, 267–282, http://dx.doi.org/10.1023/A:1006797101565.

Spencer, M., 1997. The effects of habitat size and energy on food web structure: an individual-based cellular automata model. Ecol. Model. 94, 299–316.

Stearns, S.C., 1992. The Evolution of Life Histories, vol. 249. Oxford University Press, Oxford, United Kingdom.

Stibor, H., 1992. Predator induced life-history shifts in a freshwater cladoceran. Oecologia 92, 162–165, http://dx.doi.org/10.1007/BF00317358.

Tarling, G., Burrows, M., Matthews, J., Saborowski, R., Buchholz, F., Bedo, A., Mayzaud, P., 2000. An optimisation model of the diel vertical migration of northern krill (*Meganyctiphanes norvegica*) in the Clyde Sea and the Kattegat. Can. J. Fish. Aquat. Sci. 57, 38–50, http://dx.doi.org/10.1139/f00-171.

Thorisson, K., 2006. How are the vertical migrations of copepods controlled? J. Exp. Biol. Ecol. 329, 86–100, http://dx.doi.org/10.1016/j.jembe.2005.08.011.

Threlkeld, S.T., 1976. Starvation and the size structure of zooplankton communities. Freshw. Biol. 6, 489–496, http://dx.doi.org/10.1111/j.1365-2427.1976.tb01640.x.

Unstad, K.H., Tande, K.S., 1991. Depth distribution of *Calanus finmarchicus* and *C. glacialis* in relation to environmental conditions in the Barents Sea. Polar Res. 10, 409–420, http://dx.doi.org/10.3402/polar.v10i2.6755.

Ussing, H.H., 1938. The biology of some important plankton animals in the fjords of East Greenland. In: Gunnar, T. (Ed.), Treaarsexpeditionen til Christian den X's Land 1931/34, vol. 100. Reitzel, Copenhagen, Denmark, pp. 1–20.

Uye, S., Huang, C., Onbe, T., 1990. Ontogenetic diel vertical migration of the planktonic copepod *Calanus sinicus* in the Inland Sea of Japan. Mar. Biol. 104, 389–396, http://dx.doi.org/10.1007/BF00345674.

van Haren, H., Compton, T.J., 2013. Diel vertical migration in deep sea plankton is finely tuned to latitudinal and seasonal day length. PLoS One 8, e64435, http://dx.doi.org/10.1371/journal.pone.0064435.

Varpe, Ø., Fiksen, Ø., 2010. Seasonal plankton–fish interactions: light regime, prey phenology, and herring foraging. Ecology 91, 311–318, http://dx.doi.org/10.1890/08-1817.1.

Varpe, Ø., Jørgensen, C., Tarling, G., Fiksen, Ø., 2007. Early is better: seasonal egg fitness and timing of reproduction in a zooplankton life-history model. Oikos 116, 1331–1342, http://dx.doi.org/10.1111/j.0030-1299.2007.15893.x.

Varpe, Ø., Jørgensen, C., Tarling, G., Fiksen, Ø., 2009. The adaptive value of energy storage and capital breeding in seasonal environments. Oikos 118, 363–370, http://dx.doi.org/10.1111/j. 1600-0706.2008.17036.x.

Varpe, Ø., 2012. Fitness and phenology: annual routines and zooplankton adaptations to seasonal cycles. J. Plankton Res. 34, 267–276, http://dx.doi.org/10.1093/plankt/fbr108.

Visser, A.W., Jónasdóttir, S.H., 1999. Lipids, buoyancy and the seasonal vertical migration of *Calanus finmarchicus*. Fish. Oceanogr. 8, 100–106, http://dx.doi.org/10.1046/j.1365-2419.1999.00001.x.

Vlymen, W.J., 1970. Energy expenditure of swimming copepods. Limnol. Oceanogr. 15, 348–356, http://dx.doi.org/10.4319/lo.1970.15.3.0348.

Williamson, C.E., Fischer, J.M., Bollens, S.M., Overholt, E.P., Breckenridge, J.K., 2011. Toward a more comprehensive theory of zooplankton diel vertical migration: integrating ultraviolet radiation and water transparency into the biotic paradigm. Limnol. Oceanogr. 56, 1603–1623, http://dx.doi.org/10.4319/lo.2011.56.5.1603.

Wroblewski, J.S., 1982. Interaction of currents and vertical migration in maintaining *Calanus marshallae* in the Oregon upwelling zone—a simulation. Deep Sea Res. Part A Oceanogr. Res. Pap. 29, 665–686, http://dx.doi.org/10.1016/0198-0149(82)90001-2.

Zakardjian, B.A., Runge, J., Plourde, S., Gratton, Y., 1999. A biophysical model of the interaction between vertical migration of crustacean zooplankton and circulation in the Lower St. Lawrence Estuary. Can. J. Fish. Aquat. Sci. 56, 2420–2432, http://dx.doi.org/10.1139/f99-095.

Zanakis, S.H., Evans, J.R., 1981. Heuristic optimization: why, when, and how to use it. Interfaces 11, 84–91, http://dx.doi.org/10.1287/inte.11.5.84.

Zaret, T.M., Kerfoot, W.C., 1975. Fish predation on *Bosmina longirostris*: body-size selection versus visibility selection. Ecology 56, 232–237, http://dx.doi.org/10.2307/1935317.

Zaret, T.M., Suffern, J.S., 1976. Vertical migration in zooplankton as a predator avoidance mechanism. Limnol. Oceanogr. 21, 804–813, http://dx.doi.org/10.4319/lo.1976.21.6.0804.

Zink, R.M., 2002. Towards a framework for understanding the evolution of avian migration. J. Avian Biol. 33, 433–436, http://dx.doi.org/10.1034/j.1600-048X.2002.03081.x.